ADSORPTION OF HEAVY METAL IONS FROM AQUEOUS SOLUTIONS USING A FUNCTIONAL POLYMER ADSORBENT

MOHAMAD IZZAT ARIF BIN NORDIN

BACHELOR OF SCIENCE (HONS.) CHEMISTRY WITH MANAGEMENT
FACULTY OF APPLIED SCIENCES
UNIVERSITI TEKNOLOGI MARA
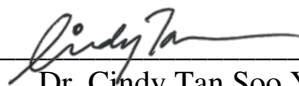
FEBRUARY 2023

ADSORPTION OF HEAVY METAL IONS FROM AQUEOUS SOLUTIONS USING A FUNCTIONAL POLYMER ADSORBENT

MOHAMAD IZZAT ARIF BIN NORDIN

**Final Year Project Report Submitted in
Partial Fulfilment of the Requirements for the
Degree of Bachelor of Science (Hons.) Chemistry with Management
in the Faculty of Applied Sciences
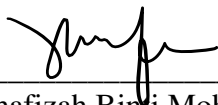Universiti Teknologi MARA**

FEBRUARY 2023

This Final Year Report Project entitled **"Adsorption of Heavy Metal Ions from Aqueous Solutions Using a Functional Polymer Adsorbent"** was submitted by Mohamad Izzat Arif bin Nordin, in partial fulfilment of the requirement for Degree of Bachelor of Science (Hons.) Chemistry with Management, in the Faculty of Applied Science, and was approved by

_____
Dr. Cindy Tan Soo Yun
Supervisor
B. Sc. (Hons.) Chemistry with Management
Center for Applied Sciences Studies
Universiti Teknologi MARA Cawangan Sarawak
93400 Kota Samarahan
Sarawak

_____
Nurhafizah Binti Mohd Selihin
Project Coordinator
B. Sc. (Hons.) Chemistry with Management
Center for Applied Sciences Studies
Universiti Teknologi MARA Cawangan Sarawak
93400 Kota Samarahan
Sarawak

_____
Ts. Dr. Siti Kartina Binti Abdul Karim
Head
Center for Applied Sciences Studies
Universiti Teknologi MARA Cawangan Sarawak
93400 Kota Samarahan
Sarawak

Date: __27 FEBRUARY 2023__

TABLE OF CONTENTS

CHAPTER 4 RESULTS AND DISCUSSION

CHAPTER 5 CONLUSION AND RECOMMENDATIONS

LIST OF TABLES

LIST OF FIGURES

aqueous environment (the circled area) compared to the still intact the P(VI-*co*-AA)/PVA network after the Cu^{2+} adsorption for 24 h. Surface cracks observed in the FESEM micrographs (a, b, f) are most likely formed during the drying of P(VI-*co*-AA) at 45 – 60°C.

LIST OF ABBREVIATIONS

AA   : Acrylic Acid

AAS   : Atomic Absorption Spectrometry

APS   : Ammonium persulphate

DN   : Double Network

DTG   : Derivative thermogravimetric

FESEM   : Field emission scanning electron microscope

FTIR   : Fourier Transform Infrared

IL   : Ionic liquid

IPN   : Interpenetrating Network

IPN   : Interpenetrating network

MBA   : Methylene bisacrylamide

NMR   : Nuclear magnetic resonance

PILs   : Poly(ionic liquid)

PVA   : Poly(vinyl alcohol)

SN   : Single Network

SPH   : Superabsorbent polymer hydrogels

TG   : Thermogravimetric

TGA   : Thermogravimetric analyzer

VI   : 1-Vinylimidazole

ABSTRACT

ADSORPTION OF HEAVY METALS IONS FROM AQUEOUS SOLUTIONS USING A FUNCTIONAL POLYMER ADSORBENT

Environmental pollution caused by untreated discharge containing heavy metal is alarming due to the toxicity. Continuous efforts in producing an economical, robust, and efficient sorbent for a variety of water pollutants such as dyes, heavy metals, microorganisms are actively being pursued. In this study, a double network polymer network consisting poly(1-vinylimidazole-*co*-acrylic acid)/poly(vinyl alcohol) (P(VI-*co*-AA)/PVA adsorbent were successfully synthesized as functional polymer adsorbent via *in-situ* free-radical polymerization followed by cyclic freeze-thaw. P(VI-*co*-AA)/PVA was characterized by using NMR, FTIR, FESEM and TGA. As a double polymer network, the swelling behaviour of P(VI-*co*-AA)/PVA adsorbent was slower and more controlled in deionized water and phosphate buffer solution at pH 7 compared to dramatic swelling of the single polymer network, P(VI-*co*-AA), which showed tendency to rupture after several hours of swelling in the aqueous media. Batch adsorption of Cu^{2+} and Pb^{2+} by the P(VI-*co*-AA)/PVA adsorbent was conducted under ambient conditions, at pH 6 and initial metal ion concentration of 100 ppm using two different adsorbent dosages until adsorption equilibria were achieved. The metal ions adsorption efficiencies of the P(VI-*co*-AA)/PVA adsorbent were compared with the single polymer networks, which were P(VI-*co*-AA) and PVA, where were prepared through similar experimental conditions. High removal efficiencies (>90%) for both Cu^{2+} and Pb^{2+} were reported for the P(VI-*co*-AA)/PVA and P(VI-*co*-AA) adsorbents at for the 1 g/L and 2 g/L adsorbents dosages, however, the P(VI-*co*-AA) network ruptured due to high osmotic pressure after several hours of adsorption. The P(VI-*co*-AA)/PVA adsorbents recorded 98 – 100 mg/g adsorption capacities (Cu^{2+} and Pb^{2+}) at 1 g/L dosage, and the adsorption capacities for these metal ions significantly reduced by ~ 50% when the adsorbent dosage was doubled whilst maintaining the initial metal ion concentration at 100 ppm. Therefore, the P(VI-*co*-AA)/PVA double-network adsorbent demonstrated enhanced mechanical properties compared to the P(VI-*co*-AA) single-network adsorbent and high adsorption capacities for Cu^{2+} and Pb^{2+}, making it as a suitable as a functional adsorbent candidate to adsorb metal ions from wastewaters.

.

ABSTRAK

PENYERAPAN ION LOGAM BERAT DARIPADA LARUTAN AKUEUS MENGGUNAKAN FUNGSIAN POLIMER PENYERAP

Pencemaran alam sekitar yang disebabkan oleh pembuangan kumbahan yang tidak dirawat yang juga mengandungi logam berat adalah bersifat toksik dan membimbangkan. Usaha beterusan dalam menghasilkan sorben yang menjimatkan, teguh dan cekap dalam pengedalian pelbahagi bahan pencemar air seperti pewarna, logam berat, mikroorganisma adalah sedang giat dijalankan. Dalam kajian ini, penjerap berasaskan jaringan polimer ganda dua yang terdiri daripada poli(vinilimidazole-*ko*-akrilik)/poli(vinil alkohol) (P(VI-*co*-AA)/PVA)) telah berjaya disinstesis sebagai penjerap berfungsi melalui proses *in-situ* pempolimeran radikal bebas diikuti dengan kitaran pencairan dan beku. Pencirian sifat bagi P(VI-*co*-AA)/PVA adalah menggunakan NMR, FTIR, FESEM dan TGA. Sebagai rangkaian polimer berganda, tingkah laku bengkak penjerap P(VI-*co*-AA)/PVA adalah lebih perlahan dan lebih terkawal dalam air ternyahion dan larutan buffer fosfat pada pH 7 berbanding dengan pembengkakan rangkaian polimer tunggal, P(VI-*co*-AA) yang dramatik, yang juga menunjukkan kecenderungan untuk bercerai selepas beberapa jam di dalam larutan akueus. Penjerapan kelompok Cu^{2+} dan Pb^{2+} oleh penjerap P(VI-*co*-AA)/PVA dijalankan dalam keadaan, pada pH 6 dan kepekatan ion logam dipermulaan pada 100 ppm dengan menggunakan dua dos penjerap yang berbeza sehingga keseimbangan penjerapan tercapai. Pembandingan Kecekapan penjerapan ion logam bagi penjerap P(VI-*co*-AA)/PVA dengan rangkaian polimer tunggal, iaitu P(VI-*co*-AA) yang terdiri daripada P(VI-*co*-AA) dan PVA juga melalui proses ekperimentasi yang sama. Kecekapan penyingkiran yang tinggi (>90%) untuk kedua-dua Cu^{2+} dan Pb^{2+} telah dilaporkan untuk penjerap P(VI-*co*-AA)/PVA dan P(VI-*co*-AA) pada untuk penjerap 1 g/L dan 2 g/L dos, bagaimanapun, rangkaian P(VI-*co*-AA) tercerai kerana tekanan osmotik yang tinggi selepas beberapa jam penjerapan. Penjerap P(VI-*co*-AA)/PVA merekodkan kapasiti penjerapan 98 – 100 mg/g (Cu^{2+} dan Pb^{2+}) pada dos 1 g/L, dan kapasiti penjerapan untuk ion logam ini berkurangan dengan ketara sebanyak ~50% apabila dos penjerap telah digandakan sambil mengekalkan kepekatan ion logam permulaan pada 100 ppm. Oleh itu, penjerap rangkaian berkembar P(VI-*co*-AA)/PVA menunjukkan sifat mekanikal yang dipertingkatkan berbanding dengan penjerap rangkaian tunggal P(VI-*co*-AA) dan kapasiti penjerapan yang tinggi untuk Cu^{2+} dan Pb^{2+}, menjadikannya sebagai penjerap yang sesuai sebagai calon penjerap berfungsi untuk menjerap ion logam daripada air sisa buangan.

ACKNOWLEDGEMENTS

Mohamad Izzat Arif Bin Nordin

CHAPTER 1

INTRODUCTION

1.1 Background

Water pollution in most developing nations arises from uncontrolled discharges of inorganic and organic pollutants, mainly heavy metals, and dyes from various sectors such as agriculture, energy production and metallurgy processes (Khurana *et al*., 2017). Effluents from the leather and textile industries often contain high concentrations of colour pigments and traces of common heavy metal ions, such as Chromium(VI), Cadmium(II), Lead(II), and Zinc(II) cations (Velusamy *et al*., 2021). Due to metal-containing dyes and complexes, heavy metals are introduced within the mechanical operation of the pre-treatment, dyeing, and finishing stages. An estimated one million metric tons of these metal-containing dyes are discharged as effluent annually (Anjaneyulu *et al*., 2005). In recent review by Yunus *et al*. (2020), the quality of coastal environment and rivers of Peninsular Malaysia deteriorates each year due to steadily increasing heavy metals contamination. It is noteworthy that heavy metals and dyes could bio-accumulate in humans through the food chain, and it is detrimental to the biota if their concentrations exceed the lethal carcinogenic and mutagenic limits (Donkadokula *et al*., 2020).

Various methods for the removal of heavy metals from wastewater have been used. This includes chemical precipitation, adsorption, membrane filtration, ion exchange, and electrochemical technologies. Adsorption is popular as one of the flexible and simple treatment methods, which results in high quality treated effluents and certain adsorbents can be reused after desorption processes (Mahmoud *et al*., 2015). Adsorption involves the adhesion of the sorbate particles to the adsorbents depending on the porosity, micro-, meso- and macropores of the adsorbent materials. These physicochemical properties of an adsorbent can be tailor-made to remove specific pollutants (Seida & Tokuyama, 2022).

A wide array of adsorbents has been studied for the removal of heavy metals from an aqueous solution, such as carbon-based, chitosan-based, mineral, magnetic, bio-adsorbent, and metal-organic frameworks (Qasem *et al*., 2021). These adsorbents have their pros and cons. The most common constraint that prevents these adsorbents from being widely used are their lack of durability, high cost and complex preparation, low selectivity towards target pollutants and inability to be recycled for sustainable and long-term applications (Vakili *et al*., 2019).

Superabsorbent polymer networks and hydrogels are used as an alternative to existing adsorbents in water treatment. Superabsorbent polymer hydrogels (SPH) are crosslinked polymeric system with a high swelling ratio (Chang *et al*., 2010). The three-dimensional mesh structure is formed via crosslinking of either natural or synthetic polymers or mixture of both (hybrid). The porous structure of the SPH allows for higher water retention and adsorption of heavy metal ions as well as other

water pollutants (Shah *et al*., 2018). Exploiting the porous structure in polymer gels will potentially increase the adsorption equilibrium and the mass transfer parameters. For instance, in a freeze-thawing of a hydrogel, a porous structure is formed when the ice crystals melt at the thawing stages (Wang & Wang, 2016). The open pores allow the dissolved ions or molecules, such as heavy metal ions to percolate deeper inside the polymer networks and gel.

The polymeric adsorbents can be functionalised with specific functional groups to act as the active adsorptive sites for targeted adsorbates via grafting, pre- or post-polymerization methods. In addition, introduction of branching to the functionalized polymers and increasing the surface area will enhance the efficiency of the adsorbent through increased number of adsorption sites (Seida & Tokuyama, 2022). Various functional moieties have been introduced to polymeric materials for different applications. The imidazole groups act as ligand for the metal chelation (Sirpa Jaaskelainen *et al*., 2020). Anionic carboxylate groups from neutralized acrylic acid (AA) can undergo metal ions exchange with its surrounding. Hence, in this study, the P(VI-*co*-AA) was synthesized via solution copolymerization of AA, 1-vinylimidazole (VI) and methylene bisacrylamide (MBA, a chemical crosslinker) in the presence of polyvinyl alcohol (PVA) to yield a semi-interpenetrating network (IPN) of P(VI-*co*-AA)/PVA. The semi-IPN P(VI-*co*-AA)/PVA was then subjected to cyclic freeze-thawing to develop a fully IPN, which is also be known as a double-network hydrogel. This double-network polymeric hydrogel is more mechanically robust and stable as adsorbents for recovery of targeted heavy metals Cu^{2+} and Pb^{2+} in a simple and efficient manner.

1.2   Problem statement

Adsorption is a technologically simple and more economically approach for wastewater treatment and a wide array of conventional (e.g activated carbons, clay minerals, zeolite, agricultural wastes, etc.) and non-conventional (e.g carbon nanotubes, metal organic frameworks, polymeric materials, hydrogels, etc.) adsorbents have been developed (Saleh, 2021). The versatility of the adsorption is largely determined by sorption capacities of the adsorbent material, which rely on the porous structures and surface property of the adsorbent. Among the major issues with the adsorption-conventional adsorbents are low adsorption capacities, poor selectivity of adsorbates/pollutants, slow adsorption kinetics, regeneration issues and sustainable management of spent adsorbents (Baskar *et al.*, 2022; Samadi *et al.*, 2021). The plastic-based sorbents are non-biodegradable and cannot be regenerated after application (Murray & Bugdayli, 2021), leading to waste accumulation, and increasing landfills.

Polymeric hydrogels are potential adsorbent materials and a good contender for treating toxic pollutants in wastewater. However, these polymer and hydrogel adsorbents, which are consisted of a single polymer network, are generally weak, soft and not mechanically robust as durable adsorbents because their 3D hydrophilic structures tend to swell excessively in aqueous solutions until their structures collapse and susceptible to dissolution, especially when these networks possess non-covalent (physical) crosslinkers and low degree of crosslinking. Moreover, physically crosslinked hydrogel networks are feebler compared to the covalently crosslinked polymeric networks. Unmodified polysaccharide hydrogels lack in

4

appropriate functional groups in the polymer networks, having mostly hydroxyl groups, thus lowering their adsorption efficiency for heavy metal ions. Functionalization of polymer networks and hydrogels with anionic and electron-rich groups can enhance the material's capacity in removing heavy-metal ions and cationic dyes present in the water.

In this study, a double network hydrogel was synthesized via *in situ* copolymerization of compatible monomers, which were AA, VI and MBA as the chemical crosslinker in the presence of dissolved PVA to form a semi-IPN consisting of a covalently crosslinked P(VI-*co*-AA)/PVA. The semi-IPN P(VI-*co*-AA)/PVA was then subjected to cyclic freeze-thawing to prepare a fully IPN or double network hydrogel. This P(VI-*co*-AA)/PVA IPN construct generally was observed to possess improved bulk mechanical properties and more controlled swellability compared to semi-IPN and single-network hydrogels. This P(VI-*co*-AA)/PVA IPN was investigated as a functional polymer-based adsorbent to adsorb model heavy metal ions (Cu^{2+} and Pb^{2+}) from a simulated wastewater.

1.3   Significance of study

Water is an essential resource for survival of all living organisms. Contaminated rivers and water supply affect the biodiversity of aquatic ecosystem, and eventually disrupt the food chain. Water remediation technologies, such as adsorption, play a vital role in removing various pollutants to ensure safe and secure water supply for humankind. Affordable, robust, efficient, and green adsorbents are highly sought-after materials for in treating wastewaters for sustainable and long-term application and management. In this study, a functional polymer adsorbent based on IPN strategy is developed via two-step facile synthesis involving *in situ* free radical polymerization followed by cyclic freeze-thaw. The IPN adsorbents were explored for adsorption of selected heavy metal ions from aqueous solutions.

1.4   Objectives and Aims

1. To synthesize a fully interpenetrating polymer network (IPN) consisting of acrylic acid (AA) and 1-vinylimidazole (VI) with poly(vinyl alcohol) (PVA) via *in situ* free radical polymerization and cyclic freeze-thaw, denoted as (P(VI-*co*-AA)/PVA).

2. To characterize the physico-chemical properties of the P(VI-*co*-AA)/PVA by using ATR-FTIR, NMR, FESEM, and TGA.

3. To investigate and compare the removal efficiency and adsorption capacity of the Cu^{2+} and Pb^{2+} of the polymer adsorbents.

CHAPTER 2

LITERATURE REVIEW

2.1   Adsorption

Adsorption is a process of mass transfer where a liquid solute (adsorbate) adheres to the active surface of a solid (adsorbent) to form a molecular or atomic film (Burakov *et al*., 2018). The adsorbate is the adsorbed solute, while the adsorbent is a solid support material (Erkey & Türk, 2021). Adsorbates and adsorbents possess particular physico-chemical properties that are influenced by constituents functional groups, porosity and etc. The presence of the residual imbalance force that attracts and retains the molecules on the adsorbate and adsorbent produces a binding force.

The binding interactions between the adsorbate and adsorbent are divided into physisorption (physical adsorption) and chemisorption, depending on their surface functionalities (Soliman & Moustafa, 2020, Gao *et al*., 2020). Physisorption and chemisorption can also occur simultaneously, where a layer of molecules may adsorb physically (or reversibly) on top of an underlying chemisorbed layer. Certain surfaces can exhibit physisorption at a lower temperature, and switch to chemisorption at a higher temperature (Webb, 2003). Physisorption occurs on all surfaces provided that temperature and pressure conditions are favourable. In

contrast, chemisorption, is highly selective and only takes place between certain adsorbate and adsorbent species after the chemically active surface is cleaned of previously adsorbed molecules (Webb, 2003). In water purification and wastewater remediation, adsorption is a common practice due to high metal uptake rates, high selectivity, and fast adsorption kinetics (Wang & Chen, 2009). On that account, adsorption is favourable method to remove hazardous substance from dilute solution. Nevertheless, adsorbents with finer pores such as zeolites and certain carbon-based adsorbent often show lower sorption rates (Erkey & Türk, 2021).

2.1.1   Physical adsorption (Physisorption)

Physisorption is the physical interactions between the adsorbent and adsorbed molecules (Khulbe & Matsuura, 2018), rarely affecting the electronic structure of the atom or molecule. The force attractions between the two molecules are the relatively weak and nonspecific Van der Waals forces such as the electrostatic interactions, ion exchange, hydrogen bonding and metal-ligand coordination (Gao *et al*, 2020), enabling the reversible adsorption to occur on any solid surfaces. Therefore, it is also regarded as Van der Waals or reversible adsorption (Deng *et al*., 2018) because the adsorbate atoms are not chemically bound to the surface atoms in the multimolecular layer formation. Generally, the physisorption involves weak and reversible binding forces, thus does not require any activation energy and high heat of adsorption.

The polymeric functional groups, such as carboxylate and imidazole, can act binding sites for metal ion adsorption via electrostatic interactions and metal-ligand coordination to form metal anion complexes. In a study of metal ion adsorption by Gao *et al.* (2020), it was reported that when a competitive chelation occurs, the strength of Van de Waals force is also influenced by the distance between the metal ions and the donor atoms of the adsorbent. Chen *et al.* (2019) observed that the lone pairs of electrons on the *N*-imidazole ring in an alternate arrangement of PVI-*g*-PS resin allowed chelation and coordination-based adsorption of Pb(II), Cu(II), Ni(II) and Cd(II) ion (Figure 2.0).
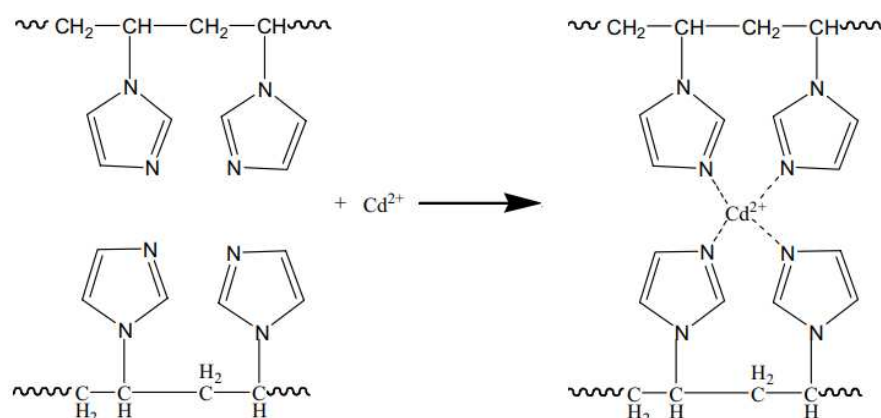
Figure 2.0 Schematic representation of adsorption mechanism of PVI-g-PS resin for Cd(II) (Chen *et al.*, 2019)

2.1.2 Chemical adsorption (Chemisorption)

Chemisorption is an adsorption involving formation of new chemical bonds between the specific active sites of the adsorbent and adsorbed molecules. The chemisorption is much stronger compared to the physisorption. Chemisorption

forms a high specific mono-molecular layer adsorption under a high temperature, adsorption heat, and activation energy (de Gisi *et al*., 2016). Unlike physisorption chemisorption only occurs on clean active sites of the adsorbents, making the molecular movement is more constrained at the surface (Erkey & Türk, 2021). Chemisorption ceases when the adsorbate molecules can no longer make direct contact with the surface. When compared to the energy requirement to free a physically bonded molecule, a chemically adsorbed molecule, which is tightly bound to the surface, needs relatively high energy infusion (Webb, 2003). Due to the higher bond strength, chemisorption is an irreversible and highly selective process (Soliman & Moustafa, 2020).

Functional adsorbents are designed and constructed to selectively adsorb pollutants depending on the type of functional groups as their active sites and their spatial layout (Seida & Tokuyama, 2022). Chen et al. (2013) synthesized the crosslinked poly(1-vinylimidazole-*co*-acrylic acid) [poly(VIm-*co*-AA)], which was a polyampholytes microgel, and a crosslinked poly(1-vinylimidazole) (PVIm) by precipitation polymerization in supercritical carbon dioxide at 14 and 20 MPa for adsorption of Cr(VI) from aqueous solutions. They observed pH and initial concentration-dependent adsorption towards Cr(VI) ions by both types of polymers. Additionally, higher crosslinker ratio in the polymer particles was observed to favour the adsorption of Cr(VI) . The Cr(VI) adsorption by poly(VIm-*co*-AA) and PVIm conforms to Langmuir and Freundlich models in the concentration range of 30 - 130 mg/L at optimized pH of adsorption (2 – 2.5). Based on their relatively high adsorption capacity (> 75 mg/g) after reusing four times, the crosslinked PVIm

and poly(VIm-*co*-AA) are promising media for the removal of Cr(VI) ions and other heavy metal ions from aqueous solution (Chen *et al*., 2013).

2.2   Adsorbents

The removal of contaminants by an adsorbent primarily depends on its physico-chemical characteristics and nature, adsorption capacity, and the concentration of the pollutant present in aqueous solutions (Pourhakkak *et al*., 2021; Singh *et al*., 2018). An ideal adsorbent should have large and specific binding sites for high selectivity, low cost and high mechanical strength. Notably, the adsorbent's ability varies based on their pore sizes, pore distribution quality and active sites or functional groups on the adsorbent surfaces (Pourhakkak *et al*., 2021; Rashid *et al*., 2021). The key functional groups attached to the adsorbent will ascertain the metal ion adsorption. Thus, chemically modified adsorbents usually have higher number of specific binding sites, leading to higher adsorption capacities than unmodified or natural adsorbents (Chakraborty *et al*., 2022). A wide variety of commercial adsorbents have been reported and they can be grouped into four categories, such as natural-based and carbon-based adsorbent, industrial by-product adsorbents and polymeric adsorbents.

Various naturally occurring materials have many potentials to be used as adsorbents and have been reported in successfully removing a wide array of pollutants, including dyes, and heavy metal ions from the wastewaters (Rashid *et*

al., 2021). Naturally derived adsorbents are considered advantageous due to their abundant availability, economic feasibility, potential for metal recovery, minimal chemical use and regenerability (de Gisi *et al*., 2016; Lindholm-lehto, 2019). Among readily accessible sorbent materials are algae, bacteria, fungus, and the by-product biomass. These sorbents can efficiently adsorb metal ions out of dilute complex solutions by sorption, which is especially evident in the cell wall structure of the sorbent. (Wang & Chen, 2009). The intricate process of sorption may involve chemisorption, complexation, metal coordination and physisorption of adsorbates (such as metal ions) on naturally occurring active sites or functional groups (Lindholm-lehto., 2019).

Agriculture residues and biomass are lignocellulosic materials consisted of carbohydrate polymers (hemicellulose and cellulose) and lignin as main structural components. Diverse structures and chemical properties make these agriculture residues an appealing alternate adsorbent (Singh *et al*., 2018). Polyphenol and polyhydroxyl groups in lignin play a major role in facilitating heavy metal ions exchange process in these materials (Bakar *et al*., 2021). Acetamide, amide, amine, amino, carboxyl, phosphate and sulfhydryl groups can also be involved in sequestration of metal ions. It is also said that lignin has a far higher affinity for metal ions than do carbohydrates. Hence, chemical functionalization of carbohydrate polymers with certain functional moieties via esterification, etherification, oxidation, or halogenation can maximize their potential in the sorption of multi-valent metal ions (Lindholm-lehto, 2019). To-date, wide array of lignocellulosic biomass, including lemon peel, orange peels, banana peels, wheat

brans, coconut coir, and pulse seed coat have been investigated for wastewater remediation (Rashid *et al.*, 2021). However, the cost-effectiveness of these adsorbents on large scale has yet to be achieved due to several shortcomings, which restricts their uses in commercial applications.

Activated carbons, mostly derived from carbonized natural materials, are the most extensively utilized adsorbents for wastewater treatment on account of their large specific surface area with a porous structure for enhanced adsorption capacity and strong adsorptivity of pollutants (Jiang *et al.*, 2019). Anthracite and bituminous coals have been the major sources for production of commercial activated carbons. Low-cost materials, which are rich in carbon content and low inorganics content, such as bamboo, tree barks and other lignocellulosic materials, are suitable to be used as a precursor for activated carbon (Saleem *et al.*, 2019), as an alternative to non-renewable coals, due to increasing global concern on environmental issues (Najafi *et al.*, 2021). Abdulrazak *et al.* (2016) reported preparation of activated carbons derived from an African palm fruit with high yield and could efficiently remove heavy metal ions, such as Cd(II), Cu(II), Ni(II) and Pb(II). However, disadvantages of activated carbon as pollutant adsorbents include high production costs, average adsorption capacity and complex thermal treament after the regeneration process. Hence, Nejadshafiee & Islami (2019) studied on chemically modified activated carbon with Fe_3O_2 nanoparticle, which resulted in high number of active sites for chemisorption. Enhancement of acidic sites and the presence of functional groups on the carbon-based adsorbents yielded an exceptional adsorption result.

Zeolites are naturally occurring microporous crystalline aluminosilicates consisting of a tetrahedral structure linked together by oxygen atoms. Zeolites could exchange cations and remove or accept water molecules without damaging the crystalline structure of zeolites (de Magalhães *et al*., 2022; Shi *et al*., 2018). Natural zeolites have been far more effective in removing heavy metal cations than phosphorus and heavy metal oxyanions due to their high negative charges (Dionisiou *et al*., 2013). Chemically and physically modified zeolites are also highly potential to be utilized for the adsorption of different pollutants.

Synthetic polymeric adsorbents are generally porous materials made from crosslinked interpenetrating polymer containing various functionalities such as ligands and charged moieties, which can interact with different types of the metal ions via coordination complexation and electrostatic interactions. For example, a ligand as the functional site of the polymer adsorbents can be introduced onto the polymer backbones through polymerization of a desired monomer with a monomeric ligand. It can also be achieved via a chemical reaction between a polymer and a low-molecular-weight molecule with a coordinating capacity (Shemshadi, 2012). Synthetic adsorbents generally have the advantages of high adsorption capacities (Sazali *et al*., 2020) and increased physical and chemical stability on account of their chemical structures (Okutucu, 2020) compared to naturally derived adsorbents. However, synthetic polymers produced from non-renewable petroleum resources tend to degrade extremely slowly, and may produce byproducts which can raise environmental concerns (Aljammal & Yuzakova, 2016; Vroman & Tighzert, 2009).

The adsorption capacity of these polymeric adsorbents can be improved by changing the structural porosity and texture as well as surface modification of polymeric adsorbents (Davidescu *et al*., 2019). It is common practice to modify polymeric adsorbent by including various polar and nonpolar functional groups onto the polymer matrix to act as the pendant groups to promote adsorbent-adsorbate interactions via different types of Van der Waals forces. Hydrogen bonding is widely used in adsorption processes given their properties of low energy and high selectivity (Davidescu *et al.*, 2019). Through hydrogen bonding with the various functional groups on the polymer network, the mobility of the adsorbate molecules or ions are restricted on the adsorbent (Wang *et al.,* 2021)

2.3   Hydrogels and polymer networks

Hydrogels, which are swollen and porous three-dimensional polymer networks, are recently developed with various chemical moieties to eliminate metal ions in contaminated waters via electrostatic forces, hydrogen bonds and metal-ligand complexation (Zheng & Wang, 2009). The hydrophilic hydrogels also feature high water absorption and retention efficiency without dissolving the 3D network (Dai *et al*., 2020). Hydrophilic functional groups (-COOH, -NH$_2$, -OH, -SO$_3$H, etc.) allow easy diffusion of solutes while forming stable complexes with the functional groups on a long polymeric chain. Hydrogels and polymer networks can be further classified according to their sources, crosslinking nature, chain composition, ionic

charge, response, size, and configuration as shown in Table 2.1 (Darban *et al*., 2022; Sighal & Gupta., 2016).

Table 2.1 Classification of hydrogels and polymers networks based on different properties (Darban *et al*., 2022; Sighal & Gupta., 2016).

Class	Subclass
Type of monomer/polymer used in hydrogel synthesis	Natural
	Synthetic
	Hybrid
Chain composition	Homopolymer
	Copolymer
	Multipolymer
Nature of crosslinking	Physical/non-covalent
	Chemical/covalent
Ionic charge	Neutral
	Anionic
	Cationic
	Ampholytic
Pore size	Nonporous
	Microporous
	Macroporous

In a synthesis of polymer and polymer networks (including hydrogels), essential components are monomers, initiator and a suitable crosslinker. The initiator initiates the polymerization of monomers in absence or presence of a crosslinking agent to form polymers and networks, respectively. A densely packed three-dimensional structure can be obtained by increasing the degree of crosslinking. Often, the number of adsorption sites and the hydrogel's swelling degree and elasticity will be reduced with increasing degree of crosslinking.

Degree of crosslinking in a polymer network regulates the water absorption while maintaining and stabilizing the polymer materials and their swelling behaviour (Bashir *et al*., 2020). Hence, an optimal degree of crosslinking must be

determined for any hydrogels and polymer networks via control of the ratio of crosslinker to monomers. It is also possible to alter the crosslinking in a polymer network with adjustment of temperature. The hydrogen-bonded networks are generally temperature-sensitive and their viscoelasticity can be altered into a low-viscosity mixture at high temperatures and more solid-like qualities at lower temperatures. This indicates that material properties can be designed by selecting the right H-bonds to produce a stimuli-responsive or smart material, in which strong H-bonds in the network structure show a retarded bond exchange, whereas weak H-bonds tend to have faster bond exchange, resulting in properties that are more solid-like (Tee *et al*., 2019).

Environmental changes involving external stimuli, such as pH, temperature, and magnetic/electrical field, affect the swelling and deswelling properties of the hydrogels and polymer networks. In a review by Sighal & Gupta (2016), cationic hydrogels are reported to exhibit superior swelling and deswelling at lower pH compared to anionic hydrogels whose swelling and deswelling properties more evident at higher pH. Acrylic acid (AA), maleic acid and *p*-styrene sulfonic acid are amongst the monomers used in anionic-based hydrogels whilst vinyl pyridine and aminoethyl methcrylate are the examples of monomers used in cationic-based hydrogels to produce stimuli-responsive hydrogels.

An interpenetrating polymer network (IPN) consists of two or more crosslinked polymer networks that are physically interwoven but not chemically linked (Silverstein, 2020). The interlocking or entanglement of the two

components/systems can increase the stability of resultant hydrogels (Wang *et al*., 2011) and the polymer networks cannot be separated, unless the chemical bonds are broken (Shivashankar & Mandal., 2012). The crosslinks hold all the polymeric chains together within a network and prevent them from slipping past or around each other. IPNs are known to possess more superior mechanical robustness than those of single-network hydrogels which are mechanically weaker with uncontrolled swelling behaviour.

Two types of IPNs, which are simultaneous and sequential IPNs, have been identified. Simultaneous IPNs are a network whereby both network precursors are mixed as they are synthesized concurrently by stepwise chain polymerization. Sequential IPNs are formed when a single network is swollen in a solution containing a monomer, initiator, and activator with or without a crosslinker. Hence, in the presence of a crosslinker, a fully-IPN is generated. In the absence of a crosslinker, where a linear polymer interpenetrates a crosslinked network, the system is called a semi-IPN (Dragan, 2014). Figure 2.1 shows the schematic representation of IPNs and double network (DN), which is also a type of IPN (Viola *et al*., 2021).

Double network (DN) hydrogels are consisted of two interpenetrating and crosslinked polymer networks (Liu *et al*., 2018), often exhibiting excellent mechanical properties and adsorption capacities for various dyes and heavy metals. A two-step polymerization technique produces DN hydrogels (Naficy *et al.,* 2013). Gong *et al*. (2003) used a two-step polymerization technique to develop DN

hydrogels consisting of poly(2-acrylamido-2-methylpropanesulfonic acid (PAMPS) as the first network and poly(acrylamide) (PAAm) as a second network. The resultant DN showed significantly enhanced mechanical properties due to strong network entanglement. Interpenetrating the first densely crosslinked but brittle primary network to the loosely crosslinked secondary network allows the absorption of external stress and achieves a strong asymmetrical gel structure. In another research by Jing *et al*. (2019), the synthesized poly(acrylic acid-*co*-acrylamide)/poly(vinyl alcohol) DN hydrogel showed self-healing properties based on dynamically reversible bonds. Unlike the single polymer networks, the DNs are reported to demonstrate excellent performance in tensile and compressive tests due to the covalent and non-covalent crosslinking which occur simultaneously in the double network, allowing the dynamic energy dissipation in the DN material upon the application of stress.
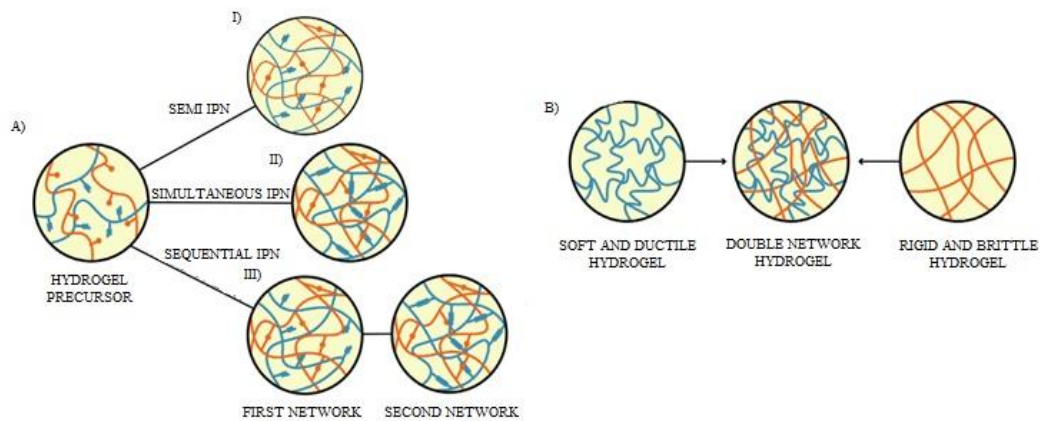
Figure 2.1   Schematic representation of A) interpenetrating polymer networks (IPNs) and B) double network (DN). The IPNs are subdivided into three types which are I) semi-IPN; II) simultaneous IPN; and III) sequential IPN (Viola *et al*., 2021).

2.4 Ionic liquids

Ionic liquid (ILs) are salts which exist in the liquid state at room temperature with a melting point of below 100°C. ILs are made up of organic cations (derivatives of *N*-substituted pyridinium, *N, N'*-substituted imidazolium, tetra-alkylated phosphonium) and other organic or inorganic anions (CF_3COO^-, HSO_4^-, Cl^-, etc.) as shown in Figure 2.2 (Singh & Savoy, 2020). Each ion in the ILs can impart a distinct functional property to a molecule, such as (1) non-volatility, which does not produce atmospheric volatile organic compound, VOCs; (2) high thermal resistance, polarity, and stability, making ILs convenient to be used in the reaction under high temperatures; (3) wide electrochemical window properties for electrochemistry; and (4) dissolution of inorganic and organic compounds and some polymers (as solvents). Hence, ILs are often regarded as green solvents and catalysts (Kosiński *et al.*, 2022; Liu *et al.*, 2010; Mallakpour & Dinari, 2012). The structure of the ionic liquids can be altered to obtain desired physical and chemical properties (Singh & Savoy, 2020)
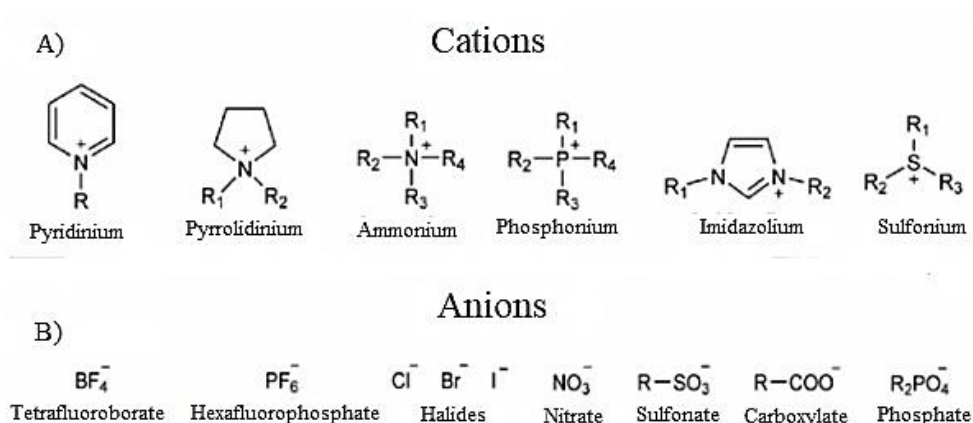
Figure 2.2 Different types of A) cations and B) anions in ionic liquids (Cruz & Ciach, 2021).

Imidazolium-based ILs are a versatile ionic liquid scaffold. The imidazolium structure is tunable to desired properties due to the inherent amphoteric behaviour, electrochemical cathodic stabilities, low melting points and low viscosities. The imidazole ring will be slightly ionized during quaternization of tertiary nitrogen atom, giving a permanent positive charge. The imidazole ring can accept and donate the protons. Since imidazole-based ionic liquid could coordinate with various alkyl substituents and counter anion, it has the potential as a water treatment agent (Green & Long, 2009). Other IL moieties are pyridinium-based and phosphonium-based ILs, which also have high degree of thermal stability (Cruz & Ciach., 2021).

2.5   Poly(ionic liquid) (PILs)

Poly(ionic liquids) (PILs) are also referred to as polymerized ionic liquids. PILs are electrolyte polymers with ionic liquid (IL) species as repeating monomer units bonded to form a polymer backbone. A new class of polymer material can be created when ILs are incorporated into the polymer chains (Yuan *et al*., 2013).

PILs are commonly synthesized through polymerization or condensation reactions (Claus *et al*., 2018). The IL monomers with poymerizable vinyl or allylic functional groups will form a unique class of PIL. This PIL may exhibit similar properties to ILs, for instance, ionic conductivity, elastic solution properties chemical and thermal stabilities. In contrast to classical polyelectrolytes, most PILs dissolve in polar organic solvents better than in an aqueous solution, thereby

22

charging the polysalt (Mecerreyes, 2011). This is due to the hydrophobicity of the counter ions and reduction of Coulombic interactions. In addition, PILs are considered mono-ionic conductors because ILs covalently interact within the polymer skeleton, limiting the mobility of the ions (Mohamed *et al.*, 2022). Contradictorily, conventional ionic polymers are not insolubilized in organic solvents.

To popularize PILs in industrial applications, the cost of PILs production should be lower compared to the current engineering plastics. Current syntheses of PILs, which involve monomeric synthesis and sequential polymerization, are rather costly. Hence, in his research, Lindner (2016) synthesized imidazolium-based polymer (polyimidazolium) via the DebusRadziszewksi reaction (excluding monomer synthesis) with high yield to lower the cost of PIL production.

Poly(*N*-vinylimidazole) (PVI) is a synthetic PIL containing a heterocyclic aromatic ring as the pendant group of the polymer (Figure 2.3a). PVI consists of a hydrophobic backbone and hydrophilic imidazole ring which can interact with other chemical groups via hydrophobic forces, hydrogen bonds and Coulombic interactions (Savin *et al.*, 2004). PVI is considered a weakly basic linear polymer which is soluble in various alcohols and aqueous solutions owing to the tertiary amine group within the PVI acting as a weak polybase when strong acids are added. Talu *et al.* (2015) reported synthesis of water-soluble poly(*N*-vinylimidazole) by radical polymerization of *N*-vinyimidazole with AIBN in 1,4-dioxane. Strong inter- and intra-molecular interactions between the imidazole rings contributed to the

tacticity of the polymer. In addition, the isotactic arrangement increases the thermal

stability of poly(*N*-vinylimidazole). There is a growing interest in PVI in a variety

of applications as catalysts and membrane materials (Fan *et al*., 2020).

2.6   Polyacrylic acid (PAA)

Polyacrylic acid (PAA) is a polyelectrolyte that is soluble in a neutral pH aqueous

solution due to ionization of the carboxylic acid at the pendant chain (Ritthidej,

2011). PAA is derived from acrylic acid (AA) monomers (Figure 2.3c), and

spontaneous polymerization of AA is highly exothermic and highly violent.
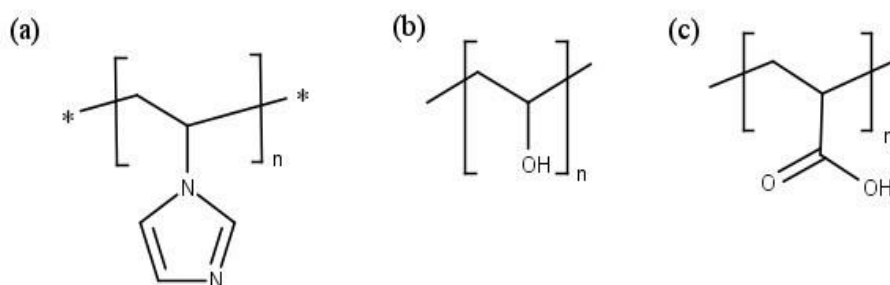
Figure 2.3   (a) Chemical structure of poly(1-vinylimidazole) (PVI); (b) poly(vinyl alcohol) (PVA); and (c) poly(acrylic acid) (PAA).

PAAs is widely utilised as a superabsorbent polymer, a dispersant, and a

scale inhibitor. PAA shows biocompatibility as a biomaterial due to its nontoxic

behaviour and biodegradable nature. Crosslinking, intermolecular cyclization or

copolymerization with another polymer may increase mechanical strength of

PAA-based materials to widen its applications in different fields (Pandey *et al*.,

2018). According to Elliot *et al*. (2004), the monomer solution concentration, pH range, and ionic strength are crucial during the polymerization of AA monomers.

2.7   Polyvinyl alcohol (PVA)

Polyvinyl alcohol (PVA) is a synthetic semicrystalline polymer (Figure 2.3b) synthesized from the hydrolysis of polyvinyl acetate (Huang *et al*., 2021). PVA can be synthesized in either free-radical polymerization of vinyl acetate (VAc) in an alcoholic solution or partial hydrolysis of poly(vinyl acetate) (PVAc) (Kumar *et al*., 2014). Due to the unstable nature of its structural monomer (vinyl alcohol), it is harder to polymerize vinyl alcohol. The partial hydrolysis of PVAc replaces the ester group of VAc with the hydroxyl group in the aqueous sodium hydroxide environment (Aslam *et al*., 2018). Manipulating external factors, such as catalyst concentration, temperature, and type of solvent used during the hydrolysis reaction, can influence the degree of hydrolysis (DH) of PVA polymer. Longer saponification reaction time and higher temperature will produce higher DH values (Alihemati & Navarchian, 2017). According to Liu *et al*. (2010), the solubility, crystallinity and chemical properties of PVA is dependent on the degree of hydrolysis. PVA is often used in industrial applications due to its high solubility, biodegradability, and biocompatibility properties.

CHAPTER 3

METHODOLOGY

3.0   Materials/Chemicals

The monomer 1-vinylimidazole (VI) (M.W 94.11) was purchased from Cool Chemical Science and Technology (Beijing) Co. Ltd. The acrylic acid (AA) (M.W 72.06), methylene biscarylamide (MBA) (M.W 154.17) and poly(vinyl alcohol) PVA (M.W 130,000) was purchased from Sigma Aldrich Canada Co. The ammonium persulphate, APS (M.W 228.20) use as polymer initiator was purchased from Thermofisher Scientific UK Co. The preparation of aqueous metal solutions was from copper (II) nitrate (M.W 241.63) and lead (II) nitrate (M.W 331.20) which were purchased from Uni-chem (UK) Co. Ltd. and Hmbg Chemical respectively. The metal standard solutions (Cu^{2+} and Pb^{2+}) used for instrumental analysis was procured from the Sigma Aldrich Germany Co. All of the experiments were carried out in deionized (DI) water.

3.1 Synthesis of Polymers and Polymers Networks

3.1.1 Partial Neutralization of Acrylic Acid (AA) Monomer

Acrylic acid (AA) was partially neutralized (60%) for this study (Figure 3.1). Predetermined amount of AA (9.14 g, 126.80 mmol) was neutralized with drops of sodium hydroxide, NaOH (8 M, 9.60 mL, 76.80 mmol) in a 50 mL round bottom flask in an ice water bath to minimize exothermic neutralization reaction heat (Ceylan *et al*., 2019). At the end of the reaction, AA solution at pH 5 - 6 was added with deionized water (DI) (6.40 mL) under continuous stirring in the ice bath.

3.1.2 Synthesis of Single-network Polymer Hydrogel, P(VI-*co*-AA)

The synthesis of P(VI-*co*-AA) is shown in Figure 3.1b. 60% neutralized AA solution in 150 mL round bottom flask was added with VI monomer (3.00 g, 31.80 mmol), followed by the crosslinking agent, methylene bisacrylamide (MBA, 0.25 g, 1.62 mmol) under constant stirring. Then DI water (64 mL) was added to the mixture in the round bottom flask. Subsequently, the mixture was purged under N_2 for 30 min at room temperature. Ammonium persulphate (APS, 0.18 g, 0.79 mmol) was added to the mixture under continuous purging of N_2 atmosphere for 15 min before being transferred it into a prepared glass mould (8 cm (W) × (11) cm (L) × 0.5 cm (thickness)) by using a micropipette. The glass mould was then sealed up and left at 70°C for 24 h. After 24 h, the hydrogel was

taken out from the mould and rinsed with copious amount of DI water and then cut

into hydrogel cubes of 1 cm × 1 cm × 0.5 cm dimension. The hydrogel cubes were

oven dried at 45°C for 24 h. Average weight of a dried single-network polymer cube

P(VI-*co*-AA) was 75.23 ± 2.28 mg.
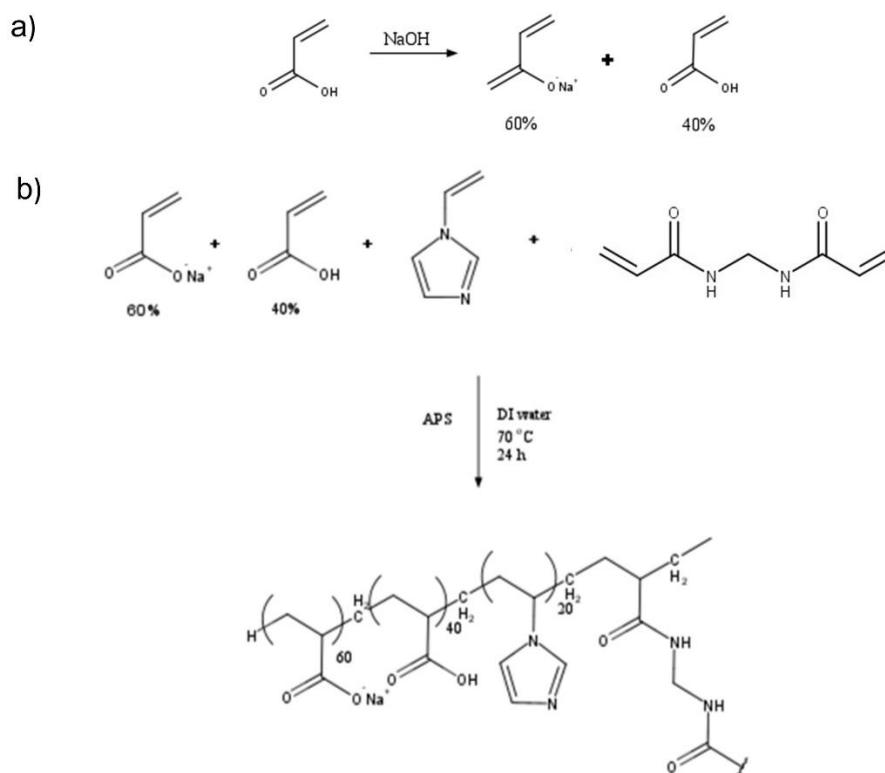
Figure 3.1.   (a) Schematic representation of partial neutralization of acrylic acid
(AA) (b) synthesis of P(VI-*co*-AA).

3.1.3 Synthesis of Double-network/IPN Polymer Hydrogel, P(VI-*co*-AA)/PVA

PVA (2.40 g, 27.90 mmol) was dissolved in DI water (30 mL) at 90°C for 24 h in a

50 mL round bottom flask under continuous stirring to completely dissolve PVA

(Byun *et al*., 2008). Then, the dissolved PVA was left to cool down before adding

other monomers. In a separate round bottom flask, the 60% neutralized AA was

added with VI (3.00 g, 31.80 mmol) followed by MBA (0.25 g, 1.62 mmol). Subsequently, the monomer mixture was added to the round bottom flask containing the viscous PVA solution. The round bottom flask was rinsed 2 - 3 times with DI water (34 mL). Total volume of the mixture was 80 mL. The mixture was purged with N_2 for 30 min before the addition of APS (0.18 g, 0.79 mmol) under constant stirring for 15 - 20 min. The mixture was purged again with N_2 for 15 min (Zhuo *et al*., 2017).

After that, the reaction mixture was transferred into the prepared glass mould, sealed, and left at $70^{\circ}C$ for 24 h. After 24 h, the polymerized product was freeze-thawed in 3 cycles (frozen at $-20^{\circ}C$ for 6 h and thawed at room temperature for 3 h) to crosslink the PVA network and form the fully IPN/double network of P(VI-*co*-AA)/PVA (Figure 3.2). The IPN hydrogels were then removed from the mould, washed with DI water, cut into hydrogel cubes of 1 cm × 1 cm × 0.5 cm dimension and were oven dried at $45^{\circ}C$ for 24 h. Average weight of a dried P(VI-*co*-AA)/PVA IPN cube was 89.28 ± 1.96 mg.
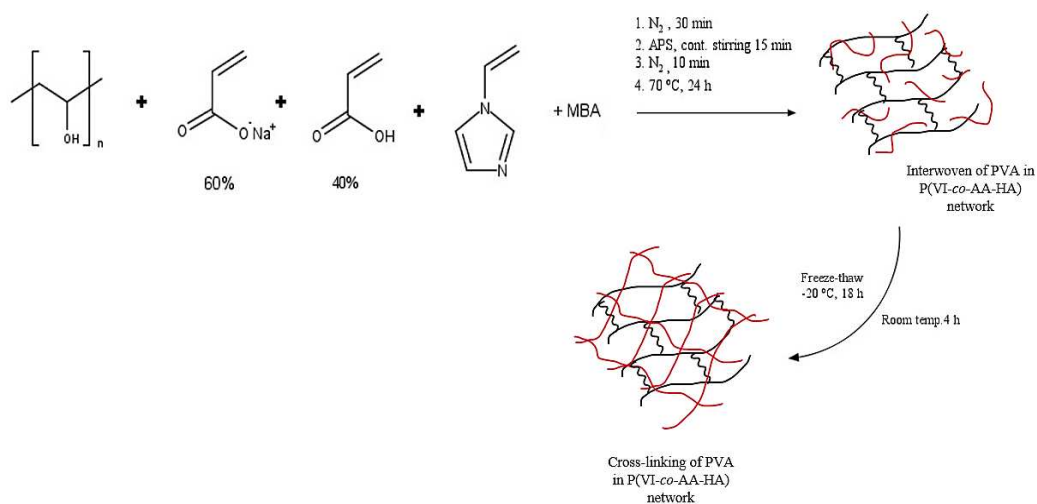
Figure 3.2   Schematic synthesis of P(VI-*co*-AA)/PVA IPN.

3.2 Characterization of Polymer and Polymer Networks

The chemical functionalities of synthesized polymers and polymer networks were analyzed by the Fourier Transform Infrared spectroscopy (FTIR, Perkin Elmer, Frontier) in the region of 4000 - 600 cm^{-1}. The P(VI-*co*-AA) was dissolved in D_2O solvent and analyzed by using NMR spectrometer (Bruker 400 MHz) at room temperature to elucidate its molecular structures. Surface morphology of dried polymer networks were observed under a Field Emission Scanning Electron Microscope (FESEM, model JEOL, JSM-IT500HR (Japan) after being sputtered with gold.

The thermal properties of the polymers were quantified by using Thermogravimetric Analyzer (TGA) (Perkin Elmer Pyris-1). In the TGA analysis, the samples were heated from 50^oC to 800^oC in a pan with heating rate of 20^oC min^{-1} under N_2 atmosphere with flowrate of 20 mL min^{-1}. The device was set at a dynamic temperature precision in the range limit of $\pm$ 0.5^oC with $\pm$ 2% of calorimetric accuracy. Thermal data was analyzed by the Pyris software. Atomic Absorption Spectroscopy (AAS) (Shimadzu Atomic Absorption AA-700) was used to quantify the concentration of metal ions adsorbed by the polymer adsorbents. Diluted aqueous solutions (dilution factor 20×) containing Cu^{2+} and Pb^{2+} from the adsorption experiments were analyzed at wavelengths of 324.8 nm, and 216.9 nm, respectively.

3.3 Swelling behaviour

The swelling behaviour of the P(VI-*co*-AA) and P(VI-*co*-AA)/PVA polymer networks, were studied and compared in two aqueous media by gravimetric method. The dried polymer adsorbents were weighed (W_d) and soaked in DI water (pH 7, 150 mL) and phosphate buffer solution (PBS, 0.1 M, pH 7, 150 mL) at room temperature consecutively until they reached equilibrium. The swollen polymeric samples were weighed (W_s) after removing excess water on the hydrogel samples with Whatman filter papers. The change in weight of adsorbent was recorded every 15 min for the first 1 h, followed by hourly for the next 5 h, 24 h, 96 h and 168 h. The equilibrium swelling ratio of the polymer adsorbent was calculated using Equation 3.1 (Wang & Wang, 2016).

$$\text{Equilibrium swelling (\%)} = \frac{(W_s - W_d)}{W_d} \times 100 \quad \text{(Equation 3.1)}$$

where, W_d = the weight of dried adsorbent and W_s = the weight of swollen adsorbent.

3.4 Adsorption Experiments

The adsorption capacity and optimal adsorbent dosage of P(VI-*co*-AA) and P(VI-*co*-AA)/PVA towards Cu^{2+} and Pb^{2+} in aqueous solutions were conducted in batch adsorption experiments. Predetermined adsorbent dosages were added to

aqueous solutions containing Cu^{2+} and Pb^{2+} ions (100 ppm, 100 mL, at 298 K) in conical flasks, separately (Table 3.1) to determine the most suitable amount of adsorbent used for adsorption kinetics and isotherm studies. The adsorbent dosage refers to the amount of adsorbent (in unit g) used per volume of solution (in unit L). The conical flasks were agitated in a mechanical shaker at 100 - 150 rpm for 24 h at room temperature. The concentration of metal ions in the supernatant were measured by using the AAS at suitable wavelengths. Standard calibration curves were constructed using standard solutions of 5, 10, 15, 20 and 25 ppm, and their best fit lines and linear regressions were analysed. Dilution was carried out to ensure that the metal ion concentration was within the limits of standard calibration curves. Each experiment was performed in triplicates under similar experimental conditions.

Table 3.1   Polymer adsorbent dosages used in the adsorption batch studies.

Dosage (g/L)	Volume of solution (mL)	Weight of adsorbent (mg)
1.0	100	100
2.0	100	200

3.5   Calculation of Removal Percentages and Equilibrium Adsorption Capacities

The removal efficiencies (%) and equilibrium adsorption capacities (q_e, in unit mg g^{-1}) of heavy metal from aqueous solutions by the polymer adsorbents was calculated based on Equations 3.2 and 3.3 (Mahmoud *et al*., 2015; Wang & Wang, 2016):

Removal efficiency, (%) = $\frac{c_o - c_e}{c_o} \times 100\%$ (Equation 3.2)

Equilibrium adsorption capacity, q_e (mg g^{-1}) = $\frac{(c_o - c_e)V}{m}$ (Equation 3.3)

where,

c_o = initial concentration of the adsorbate in solution (mg L^{-1})

c_e = equilibrium concentration of the adsorbate in solution (mg L^{-1})

q_e = adsorption capacity (mg g^{-1})

V = volume of metal ion solution (L)

m = mass of polymer adsorbent (g)

CHAPTER 4

RESULTS AND DISCUSSION

4.1 Synthesis of Polymer Networks

In this study, two types of functional polymer networks were synthesized via *in situ* free-radical polymerization in aqueous solutions in a glass mould (8 cm × 11 cm × 0.5 cm) at 70ºC for 24 – 48 h, which were single and double polymer networks. The single polymer network (SN) was consisted of a covalently crosslinked copolymer, which was poly(1-vinylimidazole-*co*-acrylic acid), denoted as P(VI-*co*-AA). Prior to the polymerization, 60% acrylic acid (AA) monomer was neutralized with NaOH, before adding 1-vinylimidazole (VI) as the comonomer, methylene bisacrylamide (MBA) as the crosslinker and ammonium persulphate (APS) as the polymerization initiator to yield a transparent yellowish hydrogel, which was quite soft and brittle. The ratio of AA to VI in the reaction mixture was 80:20.

On the other hand, the double polymer network (DN) was constructed by copolymerizing the same aqueous mixture containing 60% neutralised AA and VI monomers, MBA and APS in the presence of dissolved commercial poly(vinyl alcohol) (PVA, 3 %). A semi-interpenetrating polymer network was obtained at the end of the polymerization. It was then sent for three cycles of freeze-thaw to yield a fully crosslinked polymer network or a double network, denoted as

P(VI-*co*-AA)/PVA. The PVA network was eventually crosslinked in the cyclic freeze-thaw process. During the freezing stage, water in the semi-interpenetrating polymer network froze at -20°C, resulting in the formation of two liquid phases; a solvent-rich and a polymer-rich phase. In the polymer-rich phase, hydrogen bonding and crystallites were formed between the adjacent polymer chains (Chen *et al*., 2013) The ice formed in the solvent-phase acts as the porogen, which leads to the formation of porous structure in the solidified P(VI-*co*-AA)/PVA. The yielded P(VI-*co*-AA)/PVA DN was yellowish in colour and opaque compared to the P(VI-*co*-AA) SN due to the crosslinked PVA.

The polymer networks were taken out from the glass moulds and washed with DI water to remove unreacted monomers and other reactants. For P(VI-*co*-AA)/PVA, the polymer hydrogel was cut into cubes with a dimension 1 cm × 1 cm × 0.5 cm after washing and then dried at 45 - 60°C in the oven until constant weight. The P(VI-*co*-AA) was cut into cubes 1 cm × 1 cm × 0.5 cm after the drying for 24 h due to it fragility after washing and then were dried at 45 - 60°C until constant weight to prepare them as polymer adsorbents in the adsorption studies. Average weights of the dried P(VI-*co*-AA) and P(VI-*co*-AA)/PVA cubes were 75.23 ± 2.28 mg and 89.28 ± 1.96 mg, respectively. Figure 4.1 compares the dried P(VI-*co*-AA) and P(VI-*co*-AA)/PVA. The dried P(VI-*co*-AA) was transparent, whilst the P(VI-*co*-AA)/PVA polymer cube appeared to be opaque, with a more rigid and compact structure than the P(VI-*co*-AA). It was noted that the presence of a second network (PVA) in the adsorbent has improved the bulk mechanical strength of the P(VI-*co*-AA)/PVA.
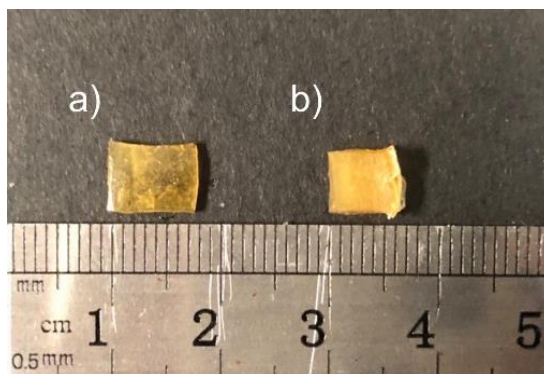
Figure 4.1 The dried (a) single polymer network, P(VI-*co*-AA); and (b) double polymer network, P(VI-*co*-AA)/PVA.

4.2   Nuclear Magnetic Resonance (NMR) Analysis

^{1}H NMR spectra were obtained by dissolving the synthesized polymers in the deuterium oxide (D_2O) solvent. The NMR results were compared between the P(VI-*co*-AA) and P(VI-*co*-AA)/PVA (Figure 4.2). In Figure 4.2a, the broad peaks at 1.00 – 2.70 ppm correspond to the H_a and H_b of the P(VI-*co*-AA) polymer backbone. The H_c peak was shifted to 4.30 ppm due to the neighbouring N-imidazole. Meanwhile, the protons of the aromatic imidazole ring (H_d, H_e, H_f) were found at around 7.30 - 7.60 ppm.
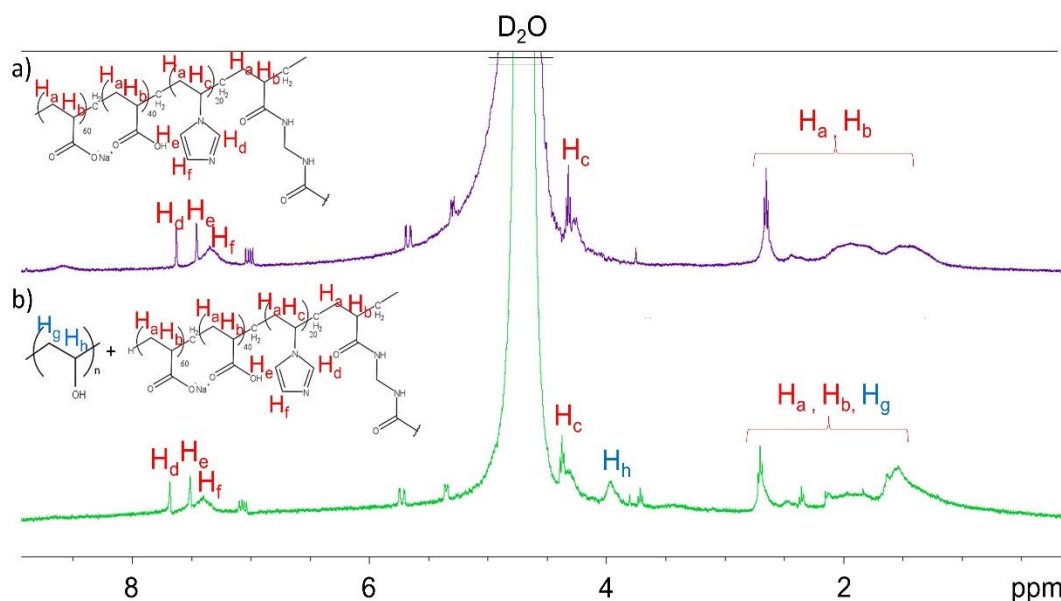
Figure 4.2 ^{1}H NMR spectra (in D_2O) and chemical structure (a) single network polymer, P(VI-*co*-AA) (b) double polymer network, P(VI-*co*-AA/PVA).

For the double network P(VI-*co*-AA)/PVA (Figure 4.2b), major proton peaks for P(VI-*co*-AA) were observed, indicating the presence of successful polymerization of P(VI-*co*-AA) in the presence of dissolved PVA. Additionally, the protons originating from PVA were found at 1.70 ppm (H_g, 2H) and 4.00 ppm (H_h, 1H), with the latter being shifted due to the hydroxyl groups. The protons from the MBA crosslinker were not noticeable as the concentration of MBA used was low (~ 0.1%). From the NMR spectra (Figure 4.2), low amounts of unreacted monomers at 5.30, 5.70 and 7.10 ppm, which most likely suggests that incomplete polymerization could have occurred. Moreover, due to the low degree of crosslinking in both hydrogels, excessive swelling of the polymer networks prevented thorough washing of the polymer networks. This dramatic swelling of the polymer network can be overcome by increasing the amount of polymerization initiator used, extending the duration of polymerization, or increasing the degree of crosslinking in the polymer networks.

4.3   Fourier Transform Infra-red (FTIR) Analysis

The IR spectra of polymer networks were obtained by using an ATR-FTIR (Figure 4.3). The IR spectrum of the single polymer network consisting of PVA only was added in Figure 4.3c for comparison purposes. The PVA single polymer network was prepared by dissolving 3% PVA in DI water, and then subjected to cyclic freeze-thaw.

The P(VI-*co*-AA) and P(VI-*co*-AA)/PVA show similar major peaks (Figure 4.3a-b). The broad bands of -OH stretching of -COOH appeared at 3349 cm^{-1} overlapping with the -NH stretching vibration of the imidazole moieties at 3100 cm^{-1}. With the -CN stretching vibration (1450 cm^{-1}) from the VI monomer, followed by the C-H ring bending vibration and -CN of the azole ring bands at 755 cm^{-1} and 623 cm^{-1}, respectively, successful copolymerization of VI and AA to form the copolymer, P(VI-*co*-AA) was shown. Moreover, the symmetrical C-H (2950 cm^{-1}) from the saturated carbon chains, the asymmetrical stretching of the C-O-C bridge (1553 cm^{-1}) and the C=O peak (1654 cm^{-1}) of the AA moieties were observed in both polymer networks (Ding *et al*., 2017; Muhammad Rapaiee *et al*., 2022).
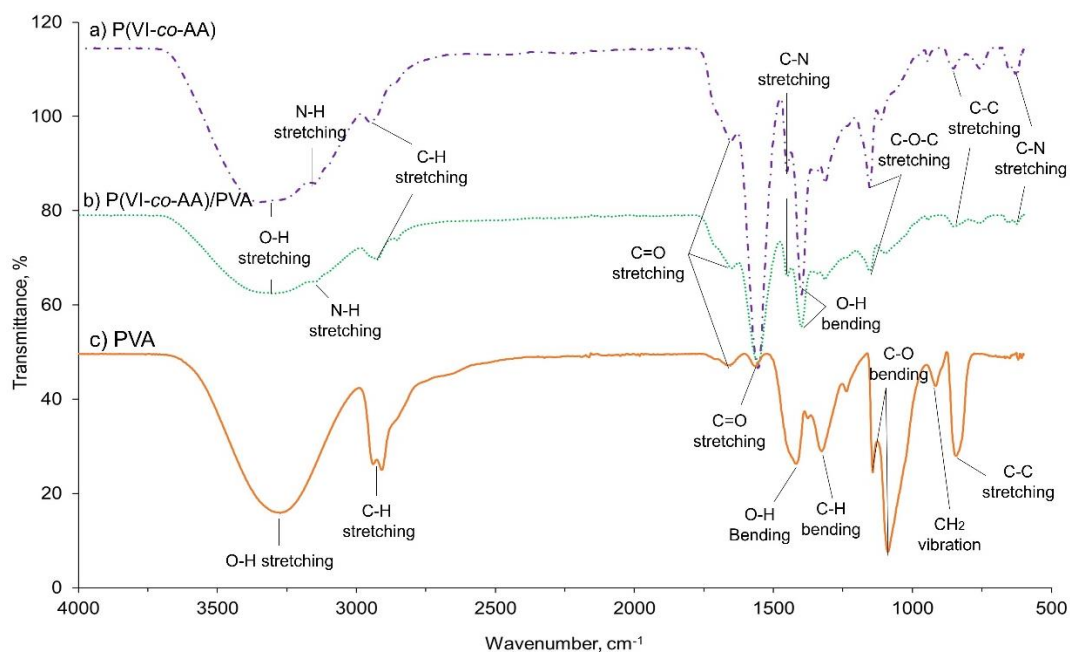
Figure 4.3   Comparison of FTIR spectra of (a) P(VI-*co*-AA); (b) P(VI-*co*-AA)/PVA; and (c) PVA polymer networks. The IR spectra for the polymers were vertically shifted by 30 unit for clarity.

Comparison of the FTIR spectra of P(VI-*co*-AA)/PVA (Figure 4.3b) and the PVA network (Figure 4.3c) shows that PVA was successfully integrated into the polymer network as the secondary polymeric network to form P(VI-*co*-AA)/PVA DN. Significant O-H (~ 3300 cm^{-1}) and C-H (2980 cm^{-1}) stretching bands from the PVA network were also observed in the P(VI-*co*-AA)/PVA network. The signals at 1100 cm^{-1} and 1380 cm^{-1} indicate the C-O stretching (of the C-O-H) and the C-H bending, while the peak at 1730 cm^{-1} was due to the C=O and C-O groups arising from residual acetate groups in the PVA network (Figure 4.3c). The presence of C-O stretching band at 1144 cm^{-1} confirms that the crystallization of PVA had taken place after the cyclic freeze-thaw process (Pour & Ghaemy, 2015; Wang & Wang, 2016; Muhammad Rapaiee *et al*., 2022) to form a single polymer network of PVA (Figure 4.3c) and double polymer network of P(VI-*co*-AA)/PVA (Figure 4.3b).

4.4   Field Emission Scanning Electron Microscope (FESEM) Analysis

The morphologies of the dried P(VI-*co*-AA) and P(VI-*co*-AA)/PVA networks were observed under FESEM at different magnifications (Figure 4.4). Based on Figure 4.4d-e, the microstructure of P(VI-*co*-AA)/PVA DN exhibited randomly distributed, deep pores and higher surface roughness and unevenness compared to the smoother and compact microstructure of P(VI-*co*-AA) SN (Figure 4.4a-b), without any noticeable pores, but more matrix cracks. The P(VI-*co*-AA)/PVA DN micropores were developed as the molecular chains of PVA and the already crosslinked P(VI-*co*-AA) network come into close proximity with one another as a result of the freezing-thawing process when ice crystals formed (Chen *et al*., 2022).

Irregular surface cracks were observed throughout the dried P(VI-*co*-AA) network (Figure 4.4a-b) before adsorption studies and in certain parts of the P(VI-*co*-AA)/PVA network, which was oven dried after the Cu^{2+} adsorption studies (Figure 4.4f). The cracks on the polymer matrixes are believed to form due to shrinkage stresses developed during the oven drying at $45 - 60^{\circ}C$. This observation implies that the mechanically weaker and softer P(VI-*co*-AA) SN is more vulnerable to shrinkage stresses compared to the mechanically more stable P(VI-*co*-AA)/PVA DN. The matrix cracks on the polymer networks could be remedied through freeze-drying (lyophilization) technique, which can also promote the formation of more porous spongelike three-dimensional structure (Lei *et al*., 2008).
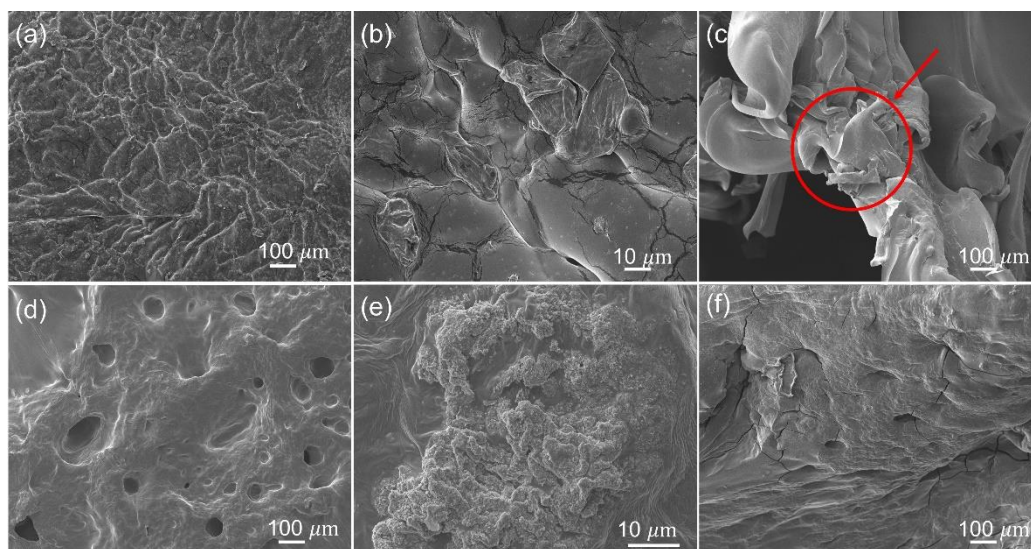
Figure 4.4   FESEM micrographs of the dried polymer adsorbents. Single-network P(VI-*co*-AA) at (a) 100×, and (b) 1000× magnification. Double-network P(VI-*co*-AA)/PVA at (d) 100×, and (e) 1000× magnification. (c) The ruptured P(VI-*co*-AA) network due to dramatic swelling in the aqueous environment (the circled area) compared to the still intact the P(VI-*co*-AA)/PVA network after the Cu^{2+} adsorption for 24 h. Surface cracks observed in the FESEM micrographs (a, b, f) are most likely formed during the drying of P(VI-*co*-AA) at 45 – 60°C.

The microstructures of P(VI-*co*-AA) and P(VI-*co*-AA)/PVA networks were also observed and compared under the microscope after 24 h adsorption studies using 100 ppm Cu^{2+} solution. It is worth mentioning that the P(VI-*co*-AA) adsorbent swelled slower during the Cu^{2+} adsorption and began to rupture from increasing osmotic pressure as well as mechanical shaking within 2 – 3 h soaking in the aqueous environment. The post-adsorption FESEM micrograph (Figure 4.4c) indicates the uneven broken edge of the dried spent P(VI-*co*-AA) adsorbent, whilst no significant structural damages were seen on the used P(VI-*co*-AA)/PVA adsorbent (Figure 4.4f).

41

4.5   Thermogravimetric analysis (TGA)

Thermogravimetric analysis was conducted from an initial temperature of 50℃ to 800℃ at the nitrogen heating rate of 20℃/min and flowrate of 20 mL/min to determine the thermal stability of the polymer networks (Figure 4.5). The TG curves of the functional polymer networks, which are P(VI-*co*-AA) and P(VI-*co*-AA)/PVA (Figure 4.5a-b) exhibited similar degradation characteristics with three distinct stages of thermal decomposition. The initial decomposition of P(VI-*co*-AA) (Figure 4.5a) occurred at a lower temperature than the P(VI-*co*-AA)/PVA network (Figure 4.5b).
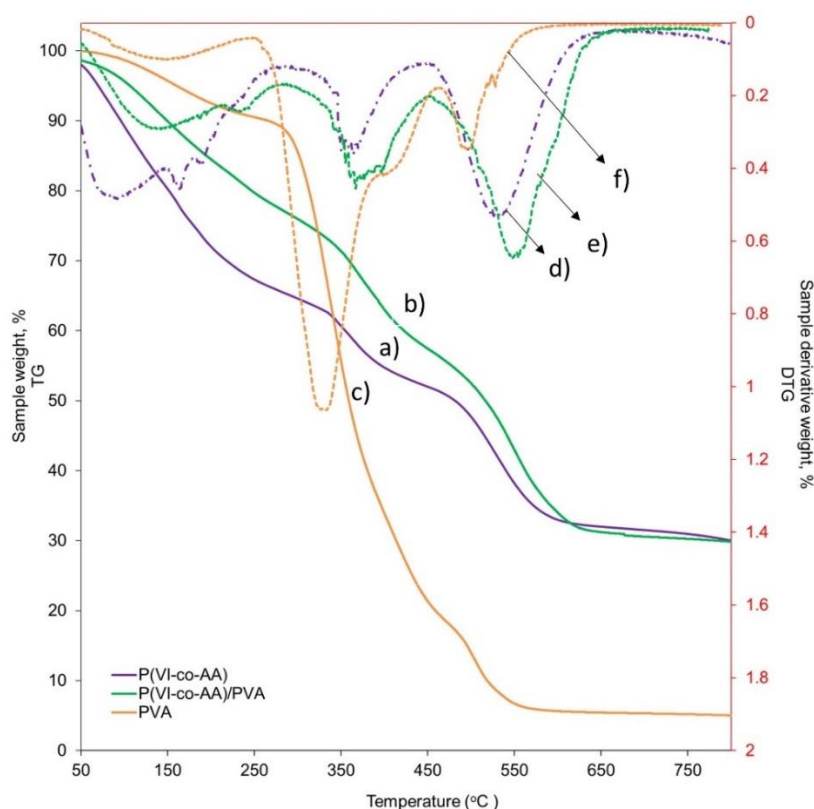
Figure 4.5   Comparison of TGA curves (denoted as solid lines, using primary y-axis) of (a) P(VI-*co*-AA), (b) P(VI-*co*-AA)/PVA and (c) PVA networks analyzed at the N_2 heating rate of 20℃ and flowrate of 20 mL/min. DTG curves for all the polymer networks (d)   P(VI-*co*-AA) (e) P(VI-*co*-AA)/PVA (f) PVA were also shown and represented using dotted lines and secondary y-axis.

The first stage of P(VI-*co*-AA) showed 36% weight loss due to moisture elimination, followed by the second decomposition at 300 - 450°C with 12.6% weight loss, which was most likely attributed to decarboxylation. In the third decomposition stage (451 - 652°C), a 20% weight loss was observed, leaving behind 32% residues attributed to further degradation of P(VI-*co*-AA) polymer, crosslinked 3D-network, imidazole moieties and other carbon-carbon bonds (Liu *et al*., 2020; Fordor *et.al* 2012). It was found that P(VI-*co*-AA)/PVA lost 27% of its initial weight at 341°C in the first decomposition stage (Figure 4.5b). The second and third stages recorded weight losses of 13% and 21%, respectively. A shift in the decomposition peak of P(VI-*co*-AA)/PVA (Figure 4.5e) was observed when compared to the TG curve of P(VI-*co*-AA) (Figure 4.d), which could be attributed to stronger intermolecular interactions, such as hydrogen bonding, between the first polymer network (P(VI-*co*-AA)) and the second polymer network (PVA) in the DN, leading to higher energy demand to break down their bonds.

In Figure 4.5c, the PVA single network also showed three stages of weight loss. In the first stage, the initial weight loss for PVA was 11% within the broad temperature range of 50 - 250°C, ascribed to moisture elimination from the freeze-thawed polymer network. Rapid degradation was observed in the second and third decomposition stages between 300°C and 550°C with weight losses around 68% and 14%, respectively, owing to the thermal decomposition of the PVA (Jadhav *et al*., 2018). The TG curve of PVA corresponds to the DTG curve (Figure 4.5f), which relates to the peak decomposition temperatures at 151°C, 342°C and 510°C.

This finding corroborates with Salh & Raswl (2018), who also reported almost similar weight losses for pure PVA.

The PVA addition in the polymer matrix to form a double network, P(VI-co-AA)/PVA, has improved its thermal stability by decreasing the rate of thermal degradation compared to the single network P(VI-co-AA). The DTG curves for both P(VI-co-AA) and P(VI-co-AA)/PVA systems in Figure 4.5d-e correspond to their respective TG curves, with the P(VI-co-AA)/PVA DN showing a shift in peak decomposition temperature to 519°C. At 800°C, both P(VI-co-AA) and P(VI-co-AA)/PVA polymer networks showed higher residue of ~ 30% compared to 5% for PVA, implying that most of the residues originated from the P(VI-co-AA) network.

4.6   Swelling Behaviour

The swelling behaviour of hydrogels and polymer networks was studied in two different media, which were DI water (Figure 4.6a) and phosphate buffer saline (PBS, Figure 4.6b) at neutral pH and ambient conditions. The PBS medium was used in this study because it is commonly used as a buffer solution in biological research.

Both P(VI-co-AA) and P(VI-co-AA)/PVA networks swelled rapidly in both aqueous media for the first 5 h of the experiments. As the single polymer network, P(VI-co-AA) showed much higher swelling rates in general compared to the double

polymer network, P(VI-*co*-AA)/PVA. The swelling percentage of P(VI-*co*-AA) in DI water peaked at 8373%, which was 4× higher than the maximum swelling percentage of P(VI-*co*-AA) in PBS (1917%) before the 3D structure of P(VI-*co*-AA) network ruptured due to dramatic swelling in an aqueous environment (Figure 4.6c-II and 4.6e-II). The swollen P(VI-*co*-AA) burst under high osmotic pressure as the network crosslinks broke, forming smaller pieces of hydrogels, resulting in substantial decreases in the swelling percentages of the P(VI-*co*-AA) network in the water environment with time due to the loss of polymeric materials.
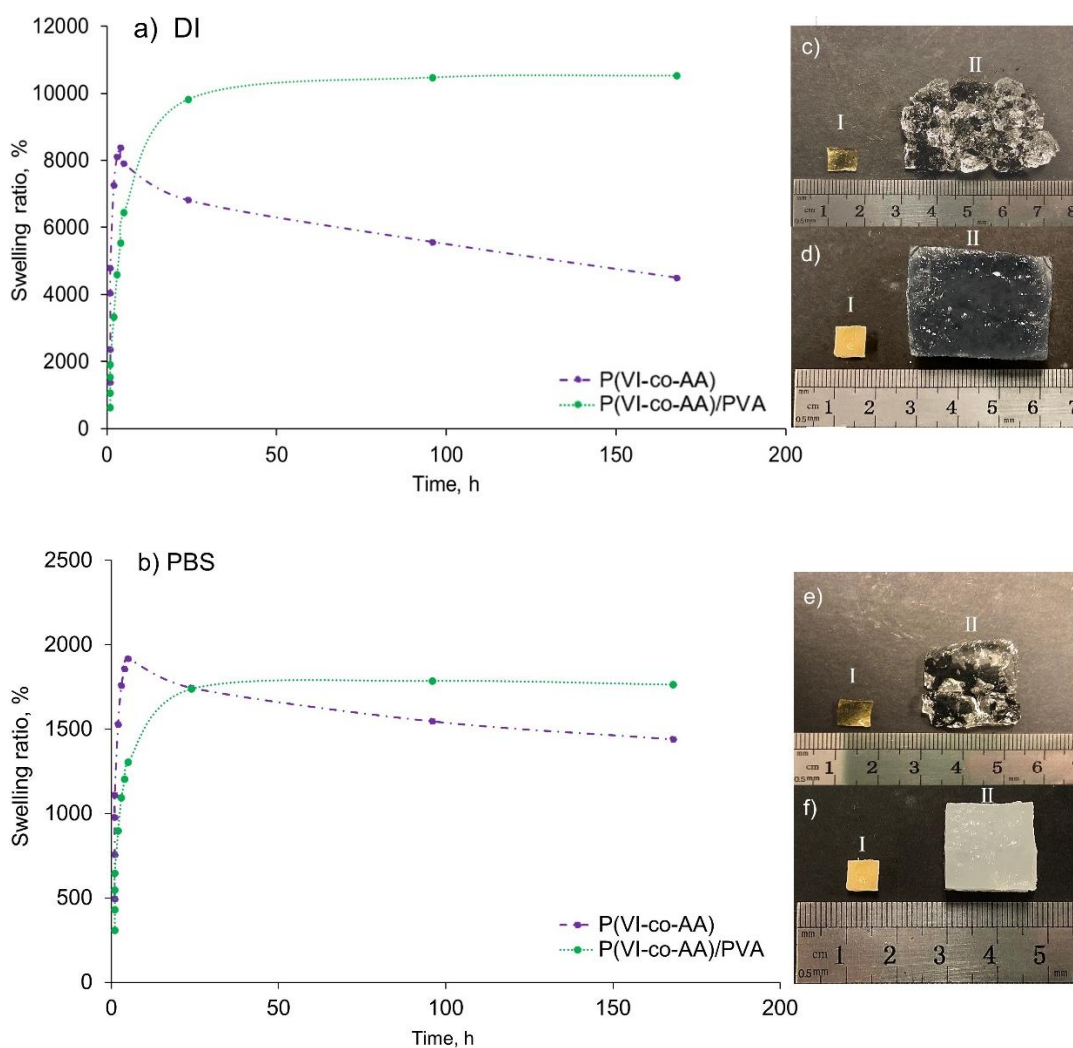
Figure 4.6   Swelling percentages of the polymer adsorbents in (a) DI water; and (b) PBS at neutral pH and room temperature for 24 h. Comparison of (c) P(VI-*co*-AA) and (d) P(VI-*co*-AA)/PVA networks before (I) and after (II) swelling experiments in DI water. Comparison of (e) P(VI-*co*-AA) and (f) P(VI-*co*-AA)/PVA networks before (I) and after (II) swelling experiments in PBS.

In contrast, it was observed that the P(VI-*co*-AA)/PVA double networks reached swelling equilibria at 9813% (in DI water) and 1738% (in PBS) after 24 h while maintaining its native structural shape (Figure 4.6d,f). Higher swelling percentages with time were also reported for P(VI-*co*-AA)/PVA compared to the P(VI-*co*-AA) single network polymer, thanks to the incorporation of hydrophilic

46

PVA network into the P(VI-*co*-AA) network to produce the stable double network. The rigid double network of P(VI-*co*-AA)/PVA exhibited some resistance to excessive swelling which could influence their utility as an adsorbent. Furthermore, hydrogen bonding between PVA and P(VI-*co*-AA) networks were likely to form in the cyclic freeze-thaw process, thus enhancing the degree of crosslinking, crystallinity, and mechanical stability of the resultant polymer network (Hassan & Peppas, 2000).

Swelling properties of a material depends on material composition (Kim & Park, 2004). Swelling rates observed in our polymer systems is most likely attributed to the presence of abundant hydroxyl, acrylate, amide and imidazole groups. These functional groups attract water molecules, which fill the inner pores within the hydrogel matrices. High water diffusion rates also cause the build-up of swelling pressure within the polymer network. When the swelling pressure reaches a critical limit of the polymer network, the crosslinks between the macromolecular chains, whether covalent or non-covalent in nature, snap and the polymer network will eventually collapse. This leads to a decrease in compressive strength of the material (Kim & Park, 2004).

4.7   Adsorption of Heavy Metal Ions

The study on the adsorbent dosage for the heavy meal adsorption allows us to optimize the adsorbent. Herein, effects of the adsorbent dosage on the adsorption

of Cu^{2+} and Pb^{2+} were investigated by using 1 g/L and 2 g/L adsorbent under room temperature conditions until an adsorption equilibrium was achieved (Figure 4.7a-b). The polymeric adsorbents were immersed and shaken in aqueous solution containing Cu^{2+} and Pb^{2+} (100 ppm, pH 6), separately, in batch-mode experiments. pH 6 was chosen based on the recommended optimal pH for the metal ion adsorption) in their metal adsorption studies (Rafatullah *et al*,. 2009)

Figure 4.7 shows the removal percentages and adsorption capacities of the heavy metals using different adsorbents and adsorbent dosages. Generally, heavy metal removal >90% was observed for the P(VI-*co*-AA) and P(VI-*co*-AA)/PVA for 1 g/L and 2 g/L adsorbents dosages. The P(VI-*co*-AA) adsorbed between 91 – 98% of Cu^{2+} and Pb^{2+} from the aqueous solutions with initial concentration of metal ion of 100 ppm. Similar adsorption efficiencies for Cu^{2+} and Pb^{2+} was recorded when the P(VI-*co*-AA)/PVA adsorbent was used, with removal percentages ranging between 92 – 99%. Basically, little variations were observed in the removal efficiencies of the two adsorbent dosages and the divalent cations, although in general, the P(VI-*co*-AA)/PVA adsorbent showed slightly higher removal percentages than the P(VI-*co*-AA) adsorbent. Based on these preliminary batch adsorption results, it is recommended to use 1 g/L adsorbent dosage for the subsequent adsorption kinetics studies.
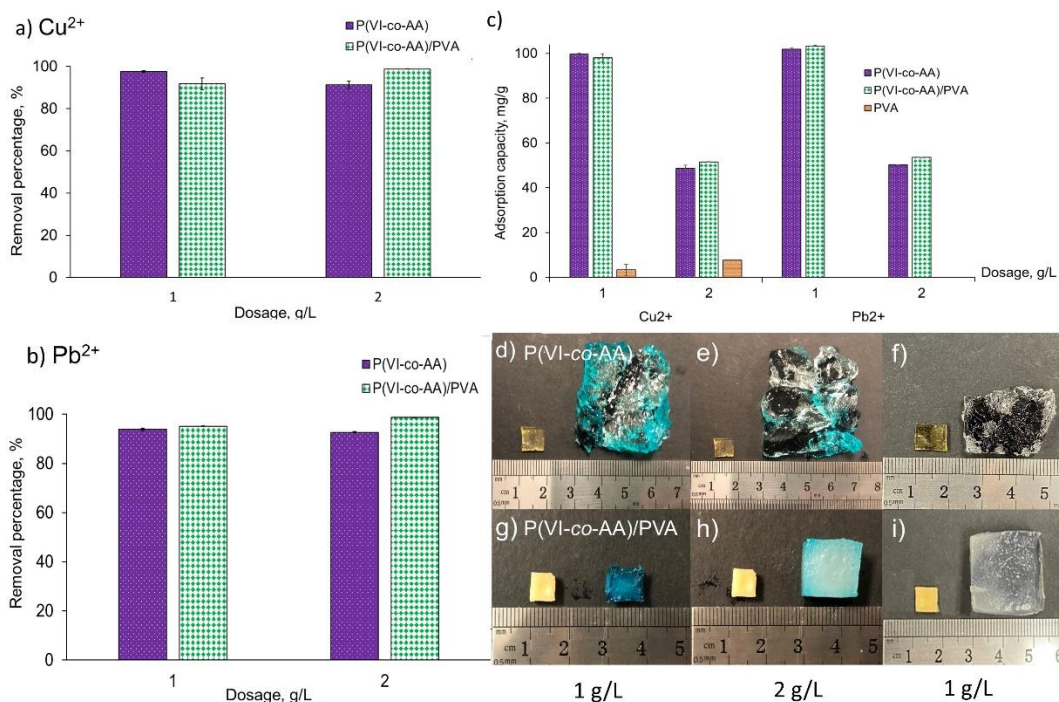
Figure 4.7   The removal percentages (%) of (a) Cu^{2+} and (b) Pb^{2+}; and the (c) adsorption capacities (q_e) of the polymer adsorbents for the metal ions by using different adsorbent dosages. Structural changes observed in the P(VI-*co*-AA) adsorbents before and after (d-e) Cu^{2+} adsorption using 1 g/L and 2 g/L adsorbents, respectively and (f) Pb^{2+} adsorption using 1 g/L adsorbents. Structural changes observed in the P(VI-*co*-AA)/PVA adsorbents before and after (g-h) Cu^{2+} adsorption using 1 g/L and 2 g/L adsorbents, respectively and (i) Pb^{2+} adsorption using 1 g/L adsorbents.

The adsorption capacities (q_e, in unit mg/g) for Cu^{2+} and Pb^{2+} by the polymer adsorbents were compared in Figure 4.7c. It is clear that the metal ion adsorption capacities of the P(VI-*co*-AA)/PVA and P(VI-*co*-AA) networks decreased with increasing amount of adsorbent used, irregardless of the type of divalent metal ion. Adsorbent dosage of 1 g/L recorded 98 – 100 mg/g adsorption capacities (Cu^{2+} and Pb^{2+}) for both adsorbents, and the adsorption capacities for these metal ions reduced by approximately 50% when the adsorbent dosage was doubled. Increasing the amount of adsorbent used also means more active binding sites are available for the metal ions. Based on our calculated removal percentages as well as the adsorption

capacities, nearly all the divalent metal ions were adsorbed by the P(VI-*co*-AA)/PVA and P(VI-*co*-AA) networks when 1g/L adsorbent dosage was used to treat the 100-ppm metal ion solutions. By increasing the adsorbent dosage to 2 g/L, while keeping the initial metal ion concentration constant at 100 ppm, complete removal of Cu^{2+} and Pb^{2+} was observed by both functional adsorbents, leaving behind ~ 50% of the active sites in the polymer adsorbent not utilized.

The adsorption efficiencies of the functional polymer networks were also compared with the single-network PVA adsorbent, which acted as control because PVA was added to the P(VI-*co*-AA)/PVA adsorbent as a support matrix only to enhance the mechanical properties of the DN adsorbent. Low Cu^{2+} adsorption capacities for the single-network PVA adsorbent were recorded at 3.34 mg/g and 7.72 mg/g for adsorbent dosage of 1 g/L and 2 g/L, respectively (Figure 4.7c). These findings indicate that the effective adsorption of the heavy metal ions rely on the active binding sites in the P(VI-*co*-AA) network, and not the PVA.

Figures 4.7d-i show the structural and colour changes of the functional polymer adsorbents before and after adsorption experiments. The adsorbents turned bluish after the Cu^{2+} adsorption and remained colourless after the Pb^{2+} adsorption (please note that the photograph's background is black). The intensity of the blue colour could also provide a qualitative estimation of the amount of adsorbed metal by the adsorbent. Due to the low mechanical strength of the P(VI-*co*-AA) adsorbent, the single polymer network suffered extreme swelling after few hours soaking in the aqueous environment, leading to structural rupture and partial

dissolution of the swollen network (Figure 4.7 d-f). In contrast, the cubic structure of the P(VI-*co*-AA)/PVA adsorbents was preserved, even under swollen states (Figure 4.7 g-i), illustrating their higher stability and integrity due to the double network assembly. Uncontrolled swelling behaviour is an unfavourable property for an adsorbent, which limits its utility in real applications because it complicates post-adsorption processing, including the separation and recovery of the metal ions and recyclability of the adsorbents for long-term uses.

The divalent metal ions, such as Cu^{2+} and Pb^{2+}, could be readily adsorbed and trapped securely within the P(VI-*co*-AA)/PVA and P(VI-*co*-AA) networks via strong electrostatic attractions, ion-dipole interactions and metal-ligand complexation (Lv *et al*., 2020; Muhammad Rapaiee *et al*., 2022), resulting in the high removal percentages at pH 6. In the P(VI-*co*-AA)/PVA and P(VI-*co*-AA) adsorbents, the ionizable carboxyl groups (R-COO⁻) of the acrylic acid could adsorb the divalent metal ions through the strong electrostatic attractions. Moreover, the COOH groups can be deprotonated into COO- in slightly acidic solutions (pH 6), which in turn provided more active binding sites for the positively charged ions (Lv. *et al*.,2019; Badsha *et al*., 2021). Metal-ligand coordination is also possible for the *N*-imidazole and COO- moieties found on the P(VI-*co*-AA) and P(VI-*co*-AA)/PVA (Badsha *et al*., 2021). Under basic conditions, imidazole can deprotonate into imidazolide anion, giving the metal ions more complexation sites. Therefore, possible adsorption mechanisms for the divalent metal ions by the P(VI-*co*-AA) and P(VI-*co*-AA)/PVA networks are chemisorption and physisorption. Chemisorption is based on electrostatic interactions and electron

exchange/sharing, whilst in physisorption, the metal ions diffuse into the pores of

the adsorbent and then deposit themselves on the surface of the adsorbent.

CHAPTER 5

CONCLUSION AND RECOMMENDATIONS

Two types of functional polymer networks, which were the single polymer network, P(VI-*co*-AA), and double polymer network, P(VI-*co*-AA)/PVA were successfully synthesized through *in situ* free-radical polymerization in aqueous solution followed by cyclic freeze-thaw. The PVA was incorporated into P(VI-*co*-AA) as the secondary matrix to improve bulk mechanical properties of the polymer network via double-network strategy. Their functional groups and chemical structures were confirmed by the FTIR and NMR analyses. Major functional groups in monomer-to-polymer conversion was high, albeit small amount of unreacted monomers were observed in the NMR spectra of the water-soluble polymers, which was most likely attributed to limited post-polymerization washing of the adsorbent. Generally, both adsorbents swelled during the washing on account of the low degree of crosslinking in the polymer structures, which eventually led to dramatic swelling of the polymer adsorbents.

FESEM micrographs show randomly distributed deep pores and rough surfaces on the P(VI-*co*-AA)/PVA network, as compared to the more compact P(VI-*co*-AA) with no visible pores but numerous matrix cracks formed from drying in the oven. Lyophilization is recommended for the drying of the polymer adsorbents to enhance the porous microstructure of the adsorbent. The TGA curves

of P(VI-*co*-AA)/PVA and P(VI-*co*-AA) showed similar characteristic temperatures of the individual polymer network with P(VI-*co*-AA)/PVA having a shift in decomposition temperature indicating that it has higher thermal stability than P(VI-*co*-AA). Investigation of the swelling characteristics of P(VI-*co*-AA)/PVA and P(VI-*co*-AA) networks in DI water and PBS (pH 7) revealed the dramatic swelling of P(VI-*co*-AA) as a single polymer network, compared to the more controlled swelling behaviour (lower swelling rates) in P(VI-*co*-AA)/PVA network. The P(VI-*co*-AA) network showed high tendency for network rupture under high osmotic pressure. Increasing the amount of polymerization initiator used, extending the duration of polymerization, or increasing the degree of crosslinking in the polymer networks is recommended to regulate dramatic swelling.

Based on the batch-mode experiments, both polymer networks exhibited high adsorption capacities for Cu^{2+} and Pb^{2+} (>90% removal efficiencies) at initial metal ion concentration of 100 ppm, surpassing the PVA adsorbent (control) at both adsorbent dosages. The adsorption capacities reduced to ~ 50 mg/g, when the adsorbent dosage was increased from 1 g/L to 2 g/L. The adsorption of the divalent cationic metals by the functional polymer adsorbent was mostly likely driven by electrostatic interactions and metal complexation (chemisorption) with the embedded functional group (acrylate and imidazole) within P(VI-*co*-AA) and P(VI-*co*-AA)/PVA.

It is recommended that adsorption kinetics and isotherm studies are carried out to determine the adsorption mechanism of divalent metal ions by the P(VI-*co*-AA)/PVA and P(VI-*co*-AA). To further understand their adsorption thermodynamics, effects of experimental parameters, such as pH and temperature during adsorption can be investigated for optimization of adsorbent purposes. The recyclability of the functional polymer adsorbent is also recommended for future studies to evaluate the economic viability and industrial utility of the polymer adsorbents.

REFERENCES

Abdulrazak, S., Hussaini, K., & Sani, H. M. (2016). Evaluation of removal efficiency of heavy metals by low-cost activated carbon prepared from African palm fruit. *Applied Water Science 2016*, 7(6), 3151–3155.

Aljammal, N., & Yuzakova, T. (2016). Review on the Effectiveness of Adsorbent Materials in Oil Spills Clean Up. *Sea*, 25(1), 36

Anjaneyulu, Y., Sreedhara Chary, N., & Samuel Suman Raj, D. (2005). Decolourization of industrial effluents - Available methods and emerging technologies - A review. *Reviews in Environmental Science and Biotechnology*, 4(4), 245–273.

Aslam, M., Kalyar, M. A., & Raza, Z. A. (2018). Polyvinyl alcohol: A review of research status and use of polyvinyl alcohol based nanocomposites. *Polymer Engineering and Science*, 58(12), 2119–2132.

Badsha, M. A., Khan, M., Wu, B., Kumar, A., & Lo, I. M. (2021). Role of surface functional groups of hydrogels in metal adsorption: From performance to mechanism. *Journal of Hazardous Materials*, 408, 124463.

Bakar, N. A., Othman, N., Yunus, Z. M., Altowayti, W. A. H., Tahir, M., Fitriani, N., & Mohd-Salleh, S. N. A. (2021). An insight review of lignocellulosic materials as activated carbon precursor for textile wastewater treatment. *Environmental Technology and Innovation,* 22, 101445

Bashir, S., Hina, M., Iqbal, J., Rajpar, A. H., Mujtaba, M. A., Alghamdi, N. A., Wageh, S., Ramesh, K., & Ramesh, S. (2020). Fundamental concepts of hydrogels: Synthesis, properties, and their applications. In *Polymers,* 12(11), 1–60

Baskar, A. V., Bolan, N., Hoang, S. A., Sooriyakumar, P., Kumar, M., Singh, L., Jasemizad, T., Padhye, L.P. & Siddique, K. H. (2022). Recovery, regeneration and sustainable management of spent adsorbents from wastewater treatment streams: A review. *Science of the Total Environment*, 153555.

Burakov, A. E., Galunin, E. v., Burakova, I. v., Kucherova, A. E., Agarwal, S., Tkachev, A. G., & Gupta, V. K. (2018). Adsorption of heavy metals on conventional and nanostructured materials for wastewater treatment purposes: A review. *Ecotoxicology and Environmental Safety*, 148, 702–712.

Byun, H., Hong, B., Sang, Y. N., Sun, Y. J., Ji, W. R., Sang, B. L., & Go, Y. M. (2008). Swelling behavior and drug release of poly(vinyl alcohol) hydrogel cross-linked with poly(acrylic acid). *Macromolecular Research*, 16(3), 189–193.

Cao, H., Duan, L., Zhang, Y., Cao, J., & Zhang, K. (2021). Current hydrogel advances in physicochemical and biological response-driven biomedical application diversity. *Signal Transduction and Targeted Therapy*, 6(1), 1–31.

Ceylan, Ö., Kaya, M. A., & Sarac, A. (2019). Preparation of partially neutralized poly(acrylic acid) microspheres via inverse pickering suspension polymerization. *Polymer Engineering and Science*, 59(1), 162–169.

Chakraborty, R., Asthana, A., Singh, A. K., Jain, B., & Susan, A. B. H. (2022). Adsorption of heavy metal ions by various low-cost adsorbents: a review. *International Journal of Environmental Analytical Chemistry*, 102(2), 342–379.

Chang, C., Duan, B., Cai, J., & Zhang, L. (2010). Superabsorbent hydrogels based on cellulose for smart swelling and controllable delivery. *European Polymer Journal*, 46(1), 92–100.

Chen, P., Cao, L., Wang, G., & Wang, J. (2013). Synthesis of cross-linked homopolymers and copolymers of 1-vinylimidazole in supercritical carbon dioxide for removal of Cr(VI) from aqueous solution. *Polymers for Advanced Technologies*, 24(8), 764–771.

Chen, Y., Li, J., Lu, J., Ding, M., & Chen, Y. (2022). Synthesis and properties of poly (vinyl alcohol) hydrogels with high strength and toughness. *Polymer Testing*, 108, 107516.

Chen, Y., Zhao, W., Yang, X., & Li, Y. (2019). Efficient removal of heavy metal ions from aqueous solution by a novel poly (1-vinylimidazole) chelate resin. *Polymer Bulletin*, 76(3), 1081–1097

Claus, J., Sommer, F. O., & Kragl, U. (2018). Ionic liquids in biotechnology and beyond. *Solid State Ionics,* 314, 119-128.

Cruz, C., & Ciach, A. (2021). Phase transitions and electrochemical properties of ionic liquids and ionic liquid—Solvent mixtures. *Molecules*, 26(12), 3668.

Darban, Z., Shahabuddin, S., Gaur, R., Ahmad, I., & Sridewi, N. (2022). Hydrogel-based adsorbent material for the effective removal of heavy metals from wastewater: A comprehensive review. *Gels,* 8(5), 263.

Davidescu, C. M., Ardelean, R., & Popa, A. (2019). New polymeric adsorbent materials used for removal of phenolic derivatives from wastewaters. *Pure and Applied Chemistry*, 91(3), 443–458.

de Gisi, S., Lofrano, G., Grassi, M., & Notarnicola, M. (2016). Characteristics and adsorption capacities of low-cost sorbents for wastewater treatment: A review. *Sustainable Materials and Technologies*, 9, 10–40.

de Magalhães, L. F., da Silva, G. R., & Peres, A. E. C. (2022). Zeolite application in wastewater treatment. *Adsorption Science and Technology*, 2020, 1-20

Deng, F., Luo, X. B., Ding, L., & Luo, S. L. (2018). Application of nanomaterials and nanotechnology in the reutilization of metal ion from wastewater. *Nanomaterials for The Removal of Pollutants and Resource Reutilization*, 149–178. Elsevier.

Ding, H., Zhang, X. N., Zheng, S. Y., Song, Y., Wu, Z. L., & Zheng, Q. (2017). Hydrogen bond reinforced poly(1-vinylimidazole-co-acrylic acid) hydrogels with high toughness, fast self-recovery, and dual pH-responsiveness. *Polymer*, 131, 95–103.

Dionisiou, N. S., Matsi, T., & Misopolinos, N. D. (2013). Phosphorus adsorption-desorption on a surfactant-modified natural zeolite: A laboratory study. *Water, Air, and Soil Pollution*, 224(1), 1-10.

Donkadokula, N. Y., Kola, A. K., Naz, I., & Saroj, D. (2020). A review on advanced physicochemical and biological textile dye wastewater treatment techniques. *Reviews in Environmental Science and Biotechnology,* 19(3), 543–560.

Dragan, E. S. (2014). Advances in interpenetrating polymer network hydrogels and their applications. *Pure and Applied Chemistry*, 86(11), 1707–1721.

Elliott, J. E., MacDonald, M., Nie, J., & Bowman, C. N. (2004). Structure and swelling of poly(acrylic acid) hydrogels: Effect of pH, ionic strength, and dilution on the crosslinked polymer structure. *Polymer*, 45(5), 1503–1510.

Erkey, C., & Türk, M. (2021). Thermodynamics and kinetics of adsorption of metal complexes on surfaces from supercritical solutions, In *Supercritical Fluid Science and Technology* , 8, 73–127.

Fan, B., Wan, J., McKay, A., Qu, Z., & Thang, S. H. (2020). Facile synthesis of wellcontrolled poly(1-vinyl imidazole) by the RAFT process. *Polymer Chemistry*, 11(35), 5649–5658.

Fodor, C., Bozi, J., Blazsó, M., & Ivan, B. (2012). Thermal behavior, stability, and decomposition mechanism of poly (N-vinylimidazole). *Macromolecules*, 45(22), 8953-8960.

Gao, X., Guo, C., Hao, J., Zhao, Z., Long, H., & Li, M. (2020). Adsorption of heavy metal ions by sodium alginate based adsorbent-a review and new perspectives. *International Journal of Biological Macromolecules*, 164, 4423-4434.

Gong, J. P., Katsuyama, Y., Kurokawa, T., & Osada, Y. (2003). Double-network hydrogels with extremely high mechanical strength. *Advanced Materials,* 15(14), 1155-1158

Green, M. D., & Long, T. E. (2009). Designing imidazole-based ionic liquids and ionic liquid monomers for emerging technologies. *Polymer Reviews*, 49(4), 291–314.

Hassan, C. M., & Peppas, N. A. (2000). Structure and morphology of freeze/thawed PVA hydrogels. *Macromolecules*, 33(7), 2472–2479.

Huang, X., Li, J., Luo, J., Gao, Q., Mao, A., & Li, J. (2021). Research progress on double network hydrogels. *Materials Today Communications*, 29, 102757.

Jadhav, V. P., Chakraborty, C. T., & Nerkar, D. M. (2018). Nanoparticle-embedded polymer reparation and characterization of PVA-PPy-Au nanocomposite free standing Films. *International Journal Scientific Research Reviews*, 7, 136-147

Jiang, C., Cui, S., Han, Q., Li, P., Zhang, Q., Song, J., & Li, M. (2019). Study on application of activated carbon in water treatment. *IOP Conference Series: Earth and Environmental Science*, 237(2), 022049.

Jing, Z., Xu, A., Liang, Y. Q., Zhang, Z., Yu, C., Hong, P., & Li, Y. (2019). Biodegradable poly(acrylic acid-co-acrylamide)/ poly(vinyl alcohol) double network hydrogels with tunable mechanics and high self-healing performance. *Polymers*, 11(6), 952.

Khurana, I., Saxena, A., Bharti, Khurana, J. M., & Rai, P. K. (2017). Removal of dyes using graphene-based composites: A review. *Water, Air, & Soil Pollution,* 228(5), 1–17.

Khulbe, K. C., & Matsuura, T. (2018). Removal of heavy metals and pollutants by membrane adsorption techniques. *Applied Water Science*, 8(1), 1–30.

Kim, D., & Park, K. (2004). Swelling and mechanical properties of superporous hydrogels of poly (acrylamide-co-acrylic acid)/polyethylenimine interpenetrating polymer networks. *Polymer*, 45(1), 189-196.

Kosiński, S., Rykowska, I., Gonsior, M., & Krzyżanowski, P. (2022). Ionic liquids as antistatic additives for polymer composites – A review. *Polymer Testing*, 107649.

Kumar, A., Negi, Y. S., Choudhary, V., & Bhardwaj, N. K. (2014). Microstructural and mechanical properties of porous biocomposite scaffolds based on polyvinyl alcohol, nano-hydroxyapatite and cellulose nanocrystals. *Cellulose*, 21(5), 3409-3426.

Lei, J., Kim, J. H., & Jeon, Y. S. (2008). Preparation and properties of alginate/polyaspartate composite hydrogels. *Macromolecular Research*, 16(1), 45-50.

Lindholm-Lehto, P. C. (2019). Biosorption of heavy metals by lignocellulosic biomass and chemical analysis. *BioResources*, 14(2), 4952-4995.

Lindner, J. P. (2016). Imidazolium-Based Polymers via the Poly-Radziszewski Reaction. *Macromolecules*, 49(6), 2046–2053.

Liu, C., Liu, H., Xiong, T., Xu, A., Pan, B., & Tang, K. (2018). Graphene oxide reinforced alginate/PVA double network hydrogels for efficient dye removal. *Polymers*, 10(8), 835.

Liu, H., Liu, Y., & Li, J. (2010). Ionic liquids in surface electrochemistry. *Physical Chemistry Chemical Physics*, 12(8), 1685–1697.

Liu, Q., Li, J., Cong, C., Cui, H., Xu, L., Zhang, Y., ... & Zhou, Q. (2020). Thermal and thermo-oxidative degradation of tetrafluoroethylene–propylene elastomer above 300° C. *Polymer Degradation and Stability*, 177, 109180.

Lv, Q., Hu, X., Zhang, X., Huang, L., Liu, Z., & Sun, G. (2019). Highly efficient removal of trace metal ions by using poly (acrylic acid) hydrogel adsorbent. *Materials & Design*, 181, 107934.

Mahmoud, A. M., Ibrahim, F. A., Shaban, S. A., & Youssef, N. A. (2015). Adsorption of heavy metal ion from aqueous solution by nickel oxide nano catalyst prepared by different methods. *Egyptian Journal of Petroleum*, 24(1), 27–35.

Mallakpour, S., & Dinari, M. (2012). Ionic liquids as green solvents: Progress and prospects. *Green Solvents II: Properties and Applications of Ionic Liquids*, 1–32.

Mecerreyes, D. (2011). Polymeric ionic liquids: Broadening the properties and applications of polyelectrolytes. *Progress in Polymer Science (Oxford)*, 36(12), 1629–1648.

Mohamed, A. H., Noorhisham, N. A., Bakar, K., Yahaya, N., Mohamad, S., Kamaruzaman, S., & Osman, H. (2022). Synthesis of imidazolium-based poly(ionic liquids) with diverse substituents and their applications in dispersive solid-phase extraction. *Microchemical Journal*, 178, 107363.

Muhammad Rapaiee, H.H., Tan, C.S.Y., Julaihi, D., Apong, H.L., Liew, F.K., Halid, Y.Y., Sim, S.F., Chiam, C-K., Than, L.T.L. (2022). Superabsorbent Interpenetrating Polymer Networks for Adsorption of Organic Dyes from Aqueous Solutions. *Malaysian Journal of Chemistry*, 24(4), 215-230.

Murray, M. L., & Bugdayli, K. (2021). Sustainable origin-sorbents for heavy metal contamination: Research progress within an Australian context. In *Sorbents Materials For Controlling Environmental Pollution*, (pp 33–48). Elsevier

Naficy, S., Kawakami, S., Sadeghovaad, S., Wakisaka, M., & Spinks, G. M. (2013). Mechanical properties of interpenetrating polymer network hydrogels based on hybrid ionically and covalently crosslinked networks. *Journal of Applied Polymer Science*, 130(4), 2504-2513.

Najafi, H., Farajfaed, S., Zolgharnian, S., Mosavi Mirak, S. H., Asasian-Kolur, N., & Sharifian, S. (2021). A comprehensive study on modified-pillared clays as an adsorbent in wastewater treatment processes. *Process Safety and Environmental Protection*, 147, 8–36.

Nejadshafiee, V., & Islami, M. R. (2019). Adsorption capacity of heavy metal ions using sultone-modified magnetic activated carbon as a bio-adsorbent. *Materials Science and Engineering: C*, 101, 42-52.

Okutucu, B. (2020). Wastewater treatment using imprinted polymeric adsorbents. *Waste in Textile and Leather Sectors.* 173-182

Pandey, S. P., Shukla, T., Dhote, V. K., Mishra, D. K., Maheshwari, R., & Tekade, R. K. (2018). Use of polymers in controlled release of active agents. *Basic Fundamentals of Drug Delivery*, 113–172.

Pour, Z. S., & Ghaemy, M. (2015). Removal of dyes and heavy metal ions from water by magnetic hydrogel beads based on poly (vinyl alcohol)/carboxymethyl starch-g-poly (vinyl imidazole). *RSC Advances*, 5(79), 64106-64118.

Pourhakkak, P., Taghizadeh, M., Taghizadeh, A., & Ghaedi, M.(2021). Adsorbent. *Interface Science and Technology*, 33(1), 71–210.

Qasem, N. A. A., Mohammed, R. H., & Lawal, D. U. (2021). Removal of heavy metal ions from wastewater: a comprehensive and critical review. *Clean Water*, 4(1), 1–15.

Rafatullah, M., Sulaiman, O., Hashim, R., & Ahmad, A. (2009). Adsorption of copper (II), chromium (III), nickel (II) and lead (II) ions from aqueous solutions by meranti sawdust. *Journal of Hazardous Materials*, 170(2-3), 969-977.

Rashid, R., Shafiq, I., Akhter, P., Iqbal, M. J., & Hussain, M. (2021). A state-of-the-art review on wastewater treatment techniques: the effectiveness of adsorption method. *Environmental Science and Pollution Research*, 28(8), 9050–9066.

Ritthidej, G. C. (2011). Nasal delivery of peptides and proteins with chitosan and related mucoadhesive polymers. *Peptide and Protein Delivery*, 47–68.

Saleem, J., Shahid, U. bin, Hijab, M., Mackey, H., & McKay, G. (2019). Production and applications of activated carbons as adsorbents from olive stones. *Biomass Conversion and Biorefinery*, 9(4), 775–802.

Saleh, T. A. (2021). Protocols for synthesis of nanomaterials, polymers, and green materials as adsorbents for water treatment technologies. *Environmental Technology & Innovation*, 24, 101821.

Salh, S. H., & Raswl, D. A. (2018). Thermal stability of polymer composite films based on polyvinyl alcohol doped with different fillers. Open Access *Journal of Physics*, 2(2), 5-10.

Samadi, A., Xie, M., Li, J., Shon, H., Zheng, C., & Zhao, S. (2021). Polyaniline-based adsorbents for aqueous pollutants removal: A review. *Chemical Engineering Journal*, 418, 129425.

Savin, G., Burchard, W., Luca, C., & Beldie, C. (2004). Global solution properties of poly(N-vinylimidazole) in ethanol. Macromolecules and aggregates. *Macromolecules*, 37(17), 6565–6575.

Sazali, N., Harun, Z., & Sazali, N. (2020). A review on batch and column adsorption of various adsorbent towards the removal of heavy metal. *Journal of Advanced Research in Fluid Mechanics and Thermal Sciences Journal Homepage*, 67(2), 66–88.

Seida, Y., & Tokuyama, H. (2022). Hydrogel Adsorbents for the Removal of Hazardous Pollutants—Requirements and Available Functions as Adsorbent. *Gels*, 8(4), 220.

Shah, L. A., Khan, M., Javed, R., Sayed, M., Khan, M. S., Khan, A., & Ullah, M. (2018). Superabsorbent polymer hydrogels with good thermal and mechanical properties for removal of selected heavy metal ions. *Journal of Cleaner Production*, 201, 78–87.

Shemshadi, R. (2012). Application of synthetic polymers as adsorbents for the removal of cadmium from aqueous solutions: Batch experimental studies. *Caspian Journal of Environmental Sciences*, 10(1), 1–8.

Shi, J., Yang, Z., Dai, H., Lu, X., Peng, L., Tan, X., Shi, L., & Fahim, R. (2018). Preparation and application of modified zeolites as adsorbents in wastewater treatment. *Water Science and Technology*, 2017(3), 621–635.

Shivashankar, M., & Mandal, B. K. (2012). A review on interpenetrating polymer network. *International Journal Pharmacy and Pharmaceutics Sciences*, 4(5), 1-7.

Silverstein, M. S. (2020). Interpenetrating polymer networks: So happy together? *Polymer*, 207(6), 3-29.

Singh, N. B., Nagpal, G., Agrawal, S., & Rachna. (2018). Water purification by using adsorbents: A Review. *Environmental Technology and Innovation*, 11, 187–240.

Singh, S. K., & Savoy, A. W. (2020). Ionic liquids synthesis and applications: An overview. *Journal of Molecular Liquids*, 297, 6-37.

Singhal, R., & Gupta, K. (2016). A review: Tailor-made hydrogel structures (classifications and synthesis parameters). *Polymer-Plastics Technology and Engineering*, 55(1), 54-70.

Sirpa Jääskeläinen, O. Koshevoy, I., Sari Suvanto, Tiina Ryhänen, & Pipsa Hirva. (2020). Vinylimidazole coordination modes to Pt and Au metal centers. *New Journal of Chemistry*, 44(29), 12762–12770.

Soliman, N. K., & Moustafa, A. F. (2020). Industrial solid waste for heavy metals adsorption features and challenges; a review. *Journal of Materials Research and Technology*, 9(5), 10235–10253.

Talu, M., Demiroğlu, E. U., Yurdakul, Ş., & Badoğlu, S. (2015). FTIR, Raman and NMR spectroscopic and DFT theoretical studies on poly(N-vinylimidazole). *Spectrochimica Acta Part A: Molecular and Biomolecular Spectroscopy*, 134, 267– 275.

Tee, H. T., Koynov, K., Reichel, T., & Wurm, F. R. (2019). Noncovalent Hydrogen Bonds Tune the Mechanical Properties of Phosphoester Polyethylene Mimics. *ACS Omega*, 4(5), 9324–9332

Vakili, M., Deng, S., Cagnetta, G., Wang, W., Meng, P., Liu, D., & Yu, G. (2019). Regeneration of chitosan-based adsorbents used in heavy metal adsorption: A review. *Separation and Purification Technology*, 224, 373–387.

Velusamy, S., Roy, A., Sundaram, S., & Kumar Mallick, T. (2021). A review on heavy metal ions and containing dyes removal through graphene oxide-based adsorption strategies for textile wastewater treatment. *The Chemical Record*, 21(7), 1570–1610.

Viola, M., Piluso, S., Groll, J., Vermonden, T., Malda, J., & Castilho, M. (2021). The Importance of Interfaces in Multi-Material Biofabricated Tissue Structures. *Advanced Healthcare Materials*, 10(21), 2101021.

Vroman, I., & Tighzert, L. (2009). Biodegradable polymers. *Materials*, 2(2), 307.

Wang, J., & Chen, C. (2009). Biosorbents for heavy metals removal and their future. *Biotechnology Advances*, 27(2), 195-226.

Wang, J., Liu, F., & Wei, J. (2011). Enhanced adsorption properties of interpenetrating polymer network hydrogels for heavy metal ion removal. *Polymer Bulletin*, 67(8), 1709–1720.

Wang, L. Y., & Wang, M. J. (2016). Removal of heavy metal ions by poly(vinyl alcohol) and carboxymethyl cellulose composite hydrogels prepared by a freeze-thaw method. *ACS Sustainable Chemistry and Engineering*, 4(5), 2830–2837.

Wang, W., Liu, X., Wang, X., Zong, L., Kang, Y., & Wang, A. (2021). Fast and highly efficient adsorption removal of toxic Pb (II) by a reusable porous semi-IPN hydrogel based on alginate and poly (vinyl alcohol). *Frontiers in Chemistry*, 9, 605.

Webb, P. A. (2003). Introduction to chemical adsorption analytical techniques and their applications to catalysis. *Micromeritics Instrument Corp. Technical Publications*, 1-12.

Yuan, J., Mecerreyes, D., & Antonietti, M. (2013). Poly(ionic liquid)s: An update. *Progress in Polymer Science*, 38(7), 1009–1036.

Yunus, K., Zuraidah, M. A., & John, A. (2020). A review on the accumulation of heavy metals in coastal sediment of Peninsular Malaysia. *Ecofeminism and Climate Change*, 1(1), 21–35.

Zheng, Y., & Wang, A. (2009). Evaluation of ammonium removal using a chitosan-g-poly (acrylic acid)/rectorite hydrogel composite. *Journal of Hazardous Materials*, 171(1– 3), 671–677.

Zhuo, Y., Liu, J., Yang, F., Li, Q., & Xing, G. (2017). Preparation and characterization of PVA/P(AA-AM) super absorbent polymer. *Integrated Ferroelectrics*, 179(1), 166– 172.

A   Personal profile

Full name	Mohamad Izzat Arif bin Nordin
National IC no	990308 13 6453
Birth date	8TH March 1999
Citizenship	MALAYSIA
Place of birth	Sarawak, MALAYSIA
Gender	Male
Correspondence address	Sublot 833, Taman Samarindah, Jalan Datuk Mohd Musa, 94300 Kota Samarahan
Telephone no. (HP)	60111 140 52297
Email address	izzat.arif0@gmail.com

B   Hobbies and interests.

As an active sociable individual, I enjoy knowing and socialising with friends and family, watching TV shows, playing computer games and reading fictional and non-fictional related books. Cleaning, organising and tidying tasks is my spirit lifters whenever stress is hitting.

C   Academic qualifications

Degree	Area	Institution	Year awarded
B.Sc. (Hons.)	Chemistry with Managaement	Universiti Teknologi MARA, Malaysia	2023
Diploma	Science	Universiti Teknologi MARA, Malaysia	2019
S.P.M	Science	Sek Berasrama Penuh Kuching Utara, Sarawak	2017

D   Related experience

Post	Place	Year
Vice Treasurer	CHEMIST, Universiti Teknologi Mara, Sarawak, Malaysia.	2022
Participant	International Conference InnoStre	2022
Committee	Inbound-Outbound Mobility program Japan-Malaysia	2022
Committee	Karnival Kimia 2022 State level	2022
Higher committee	CHEMIST, Universiti Teknologi Mara Sarawak, Malaysia	2021

E   Awards

Type	Name of award/ awarding organisation	Date
Certificate	Dean's List Award 2020, Universiti Teknologi Mara, Sarawak, Malaysia.	2020

| Certificate | Dean;s List Award 2021, Universiti Teknologi Mara Sarawak, Malaysia. | 2021 |
| Certificate | Deans's List Award 2022, Universiti Teknologi Mara Sarawak, Malaysia | 2022 |

F   Other Relevant Information